DESIGN AND PERFORMANCE ANALYSIS OF RADIO FREQUENCY MEANDERED-LINE MICROSTRIPS

BY

YIXUAN ZHAO

THESIS

Submitted in partial fulfillment of the requirements
for the degree of Bachelor of Science in Electrical and Computer Engineering
in the College of Engineering of the
University of Illinois at Urbana-Champaign, 2016

Urbana, Illinois

Adviser:

Professor José E. Schutt-Ainé

Abstract

In the design of miniature microstrip transmission lines, a meandered line is often used as an effective method to insert proper electrical delay while reducing the feature size. However, this design technique also introduces undesirable noise to the applied network. In order to provide detailed analysis regarding the electrical response from variously shaped meandered lines, eight different structures of meandered line microstrip, all of the same physical length of 125 mm, were designed, modeled and characterized in terms of their electrical properties and footprints. Both the simulations and measurements of these microstrip lines were carried out in a frequency range of 50 MHz to 10 GHz. In addition, this thesis compares the eight designs' insertion losses and discusses the possible relationship between particular structures of meandered lines and their corresponding frequency responses.

Keywords: RF/ microwave, meandered, microstrip, insertion loss

To Prof. José E. Schutt-Ainé, Xu Chen and Thong Nguyen,

for their generous mentorship and support.

TABLE OF CONTENTS

CHAPTER 1 INTRODUCTION

1.1 Motivation

With an increasing demand for size reduction of two-dimensional patterns on multilayered printed circuit boards (PCBs), the meandered line has became an essential component in most integrated microstrip line designs [1]. Over the years, much work has been contributed to match the meandered-line section to its straight-line correspondent [2], [3]. Yet, there were not as many studies dedicated to thoroughly examining and explaining how particular design parameters of the meandered line affect the overall performance of the network. Thus, it is imperative to provide an explicit review of the varied parameters of a meandered line and their corresponding effects on the microstrip's insertion loss.

1.2 Design Outline

In Chapter 2, the original meandered line microstrip M3 design in Figure 1.1 is measured and modeled with several different approaches (Figure 1.2). The data sets obtained are then compared and used to select the most accurate measurement method and the simulation method.

In Chapter 3, the eight varied shapes of the meandered lines are described and modeled in HFSS Designer. The S-parameters (including phase and magnitude) are extracted with a adaptive liner frequency sweep from 50 MHz to 10 GHz.

In Chapter 4, each of the above structures is integrated and fabricated on a FR-4 substrate with a copper ground plane. The PCBs are measured on a vector network analyzer (VNA) with full 2- port SOLT calibration. The measured insertion loss, along with the simulation results, are compared and analyzed.

In Chapter 5, conclusion of the thesis is drawn and future work on more accurate HFSS simulation of the meandered lines is discussed.

Figure 1.1 Original meandered line microstrip M3

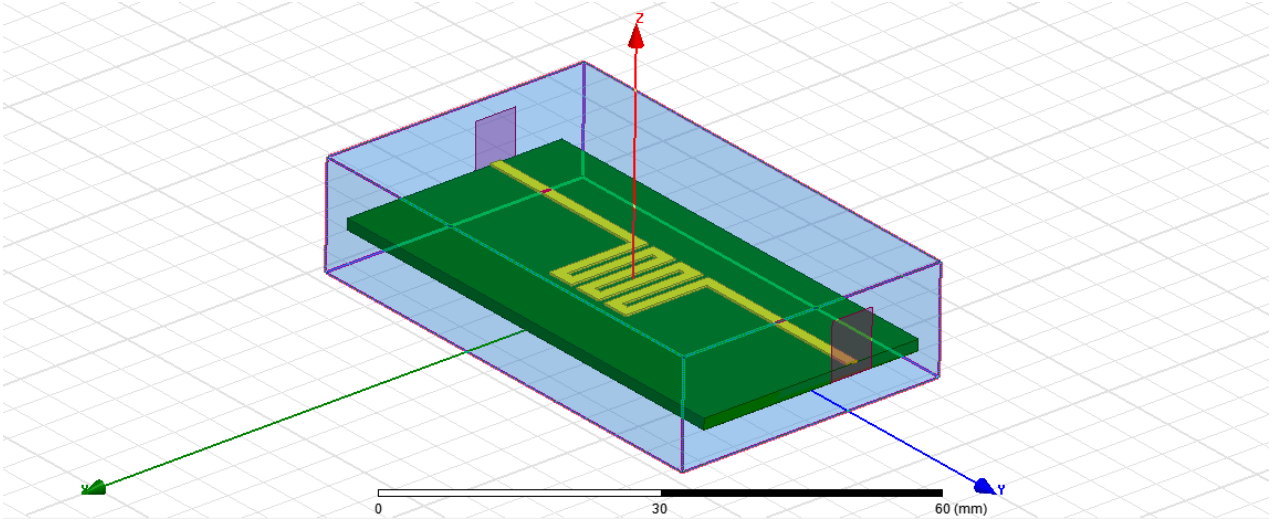

Figure 1.2 Modeling of the original meandered line microstrip M3 in HFSS

CHAPTER 2 BASIC EM STRUCTURE CHARACTERIZATION

2.1 Finite Element Method

The finite element method (FEM) for electromagnetics divides a complex problem into a finite number of pieces and solves the boundary value equations for these smaller elements [4]. In the commercial electromagnetic structure solver from Ansys, this process of mesh generation was pre-integrated and generally automatically performed. In this thesis, HFSS (High Frequency Structural Simulator) Designer [5] was selected to construct the 3D components of the meandered line microstrip by assembling numbers of stacked up layers. In addition, the HFSS 3D Layout also allows the user to view the entire structure from the top view and every layer can be edited to fit into certain geometries.

The model of the original M3 was built with the following procedure. The thickness of each layer (ground, substrate, signal line) was assigned in the stack up editor as 35 μm, 1.4 mm and 35 μm from bottom to top (Figure 2.1). Next the materials were specified. The substrate used was FR-4 with relative dielectric constant of 4.2 and the conducting layer used was the standard 1-ounce copper as shown in Table 2.1. After switching the view to the top of the structure (signal level), the meandered line was drawn by calculating the coordinates of each turning corner. When one section of the meandered part was properly placed, the rest of the model could be obtained by mirroring the existing shape 4 times. The finished model was then assigned with the 2 wave ports on the ends of the signal line by the edge selecting command. Figures 2.2 and 2.3 show the top-level view and the 3D view respectively.

Table 2.1 Design Parameters of the original meandered line microstrip M3

Dielectric Material	FR-4
Dielectric Thickness	1.4 mm
Relative Dielectric Constant	4.32 at 5 GHz
Subtract Length X Width	60 mm × 30 mm
Ground & Signal Plane Material	1.oz Copper
Ground & Signal Plane Thickness	35 μm
Conductor Width	1.4 mm
Gap Width	0.9 mm
Total Signal Line Length	125 mm

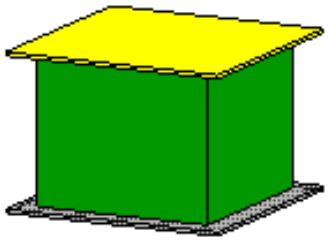

Figure 2.1 Stack up view of M3 in HFSS Designer

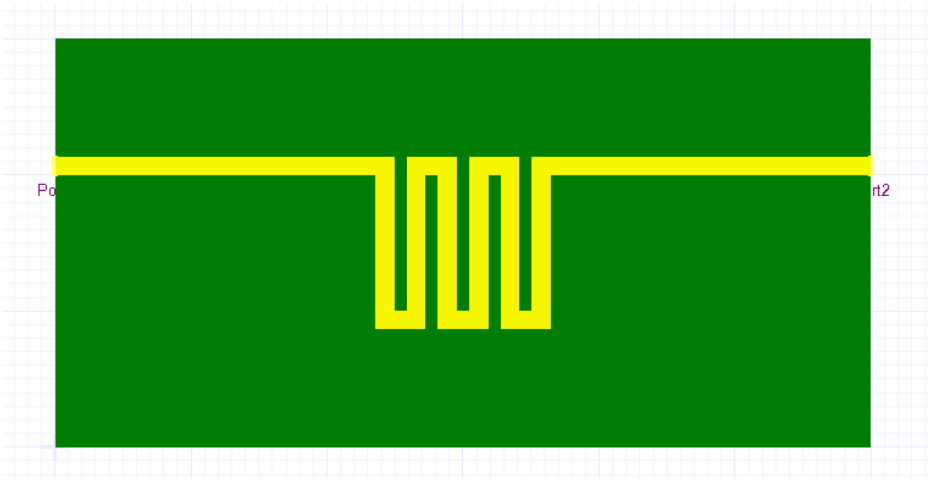

Figure 2.2 Top-level view of M3 in HFSS Designer

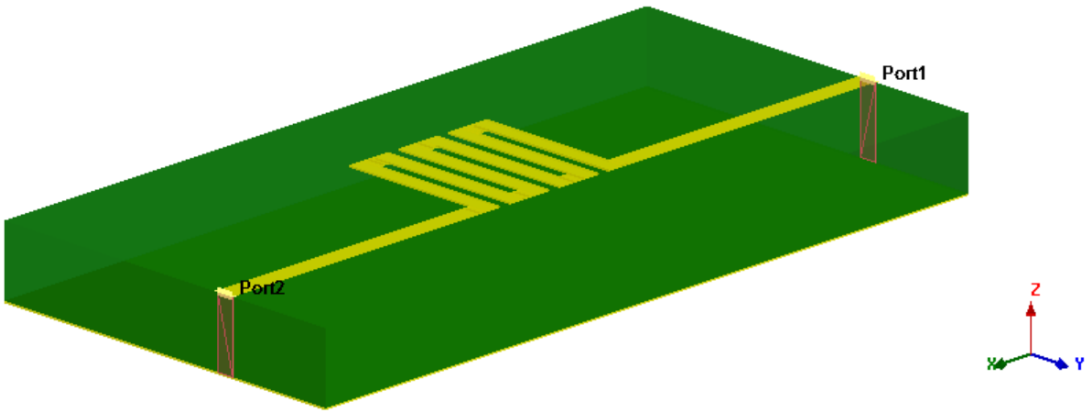

Figure 2.3 3D view of M3 in HFSS Designer

The simulation frequency applied is the adaptive passes method with a linear sweep of 50 MHz to 10 GHz. The resulting graphs are displayed in Figure 2.4. Observing from the S_{11} plot, the return loss is -25 dB at 4 GHz and keeps increasing in the higher frequency region. From the S_{21} plot, the device's insertion loss is considerably small until it reaches 4.5 GHz, indicating that this microstrip can only function below 4 GHz before suffering from too much noise.

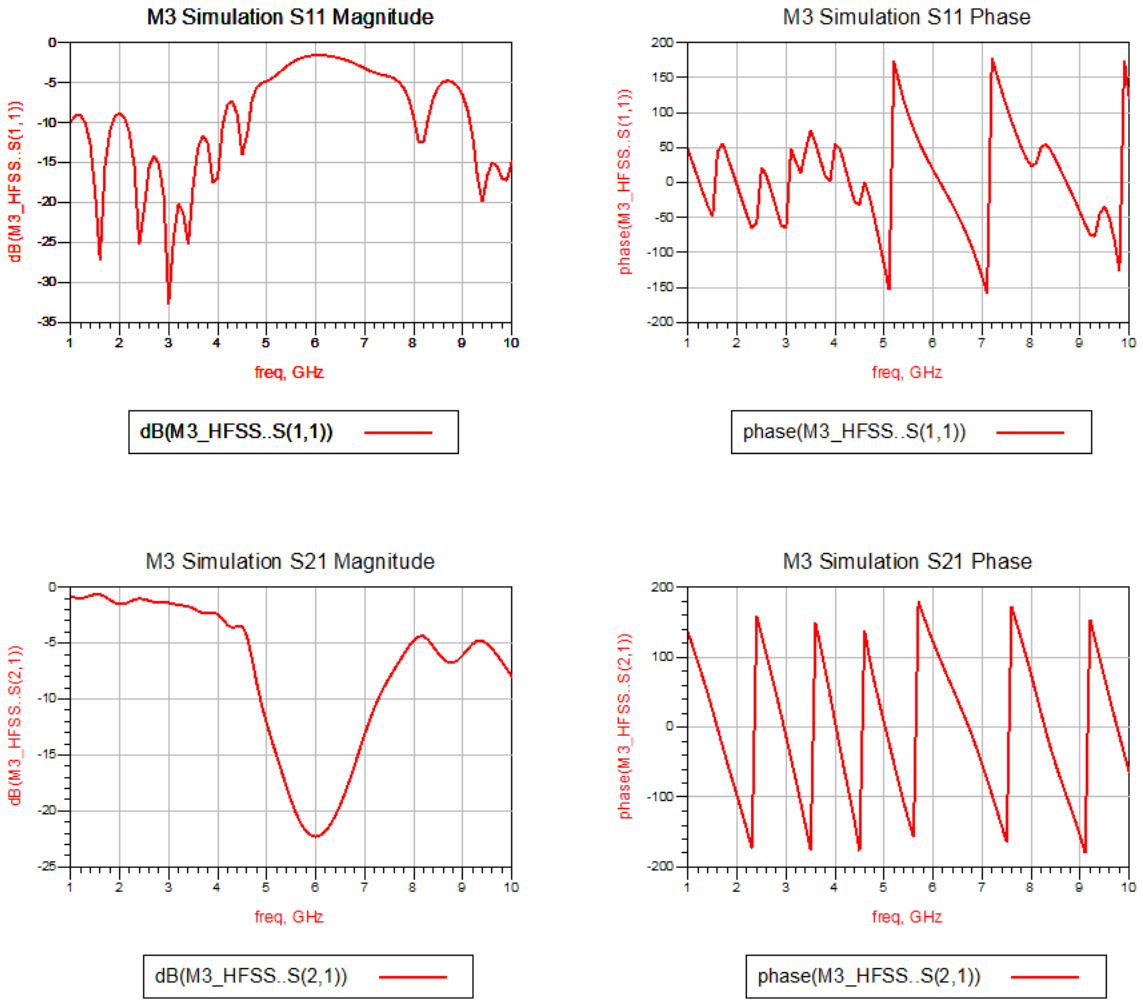

Figure 2.4 S–Parameters of M3 simulated by HFSS Designer

2.2 Shielded Domain Method

Similar to HFSS Designer mentioned above, model construction in Sonnet [6] was also done by stacking up the desired layers. The slight advantage of Sonnet was that it did not strictly require the user to calculate and enter the exact coordinates for the structure manually before plotting. Sonnet then creates a mesh by diving the geometry to either staircase or conformal subsections.

In terms of geometry building, Sonnet has its own convention for the locations of each layer (Figure 2.5). For instance, in the stack up manager, layers named GND (ground), 0 (signal) and TOP (air box top) will always be pre-specified for the user. To build the meandered line microstrip, the dielectric layer between GND and 0 plan must be assigned as the FR-4 substrate with a relative dielectric constant of 4.2 and a height of 1.4 mm. The layer between 0 and TOP is for the design of the air box (ε_r =1, 7 mm). The plane sizes (X & Y) of the air box and substrate were both found in a different panel, the box size. In that panel, one could also control the precision of the drawing using the cell size, which changes the smallest increment length in a design. Next, to add the copper layers into the design, a metal rectangle of size 60 mm × 30 mm was drawn at the GND layer and the meandered line at the 0 layer. To the user's great convenience, the meandered shaped line was pre-stored in the software under Tool > Metallization. After entering the attributes (e.g. number of legs, conductor lengths, etc.), the meandered section of the signal line would automatically be added to the conducting layer. The complete model is shown in Figures 2.6 and 2.7 for 2D and 3D views, respectively, with a centered signal layer and 2 wave ports assigned.

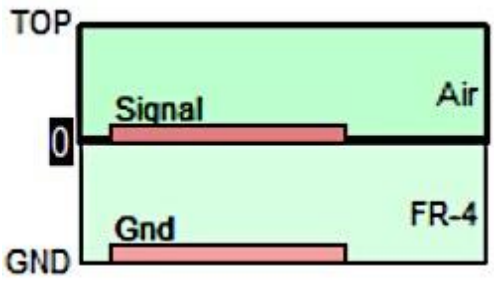

Figure 2.5 Stack up view of M3 in Sonnet

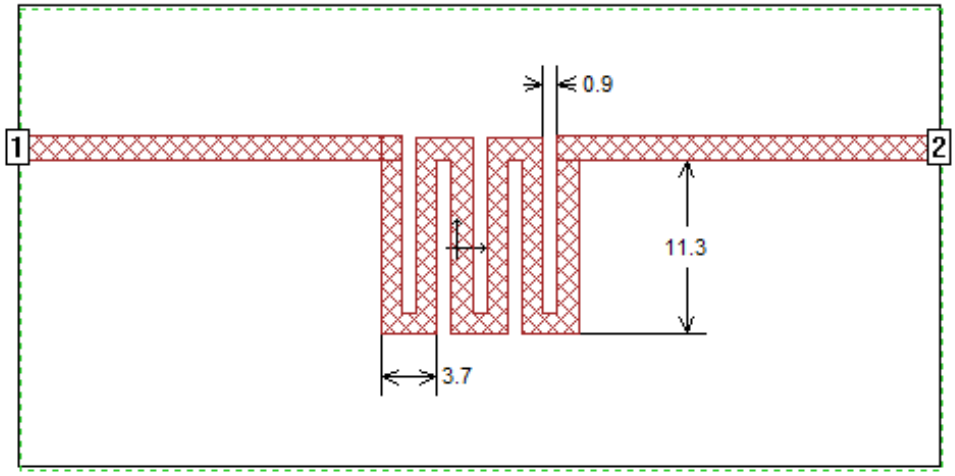

Figure 2.6 Top-level view of M3 in Sonnet

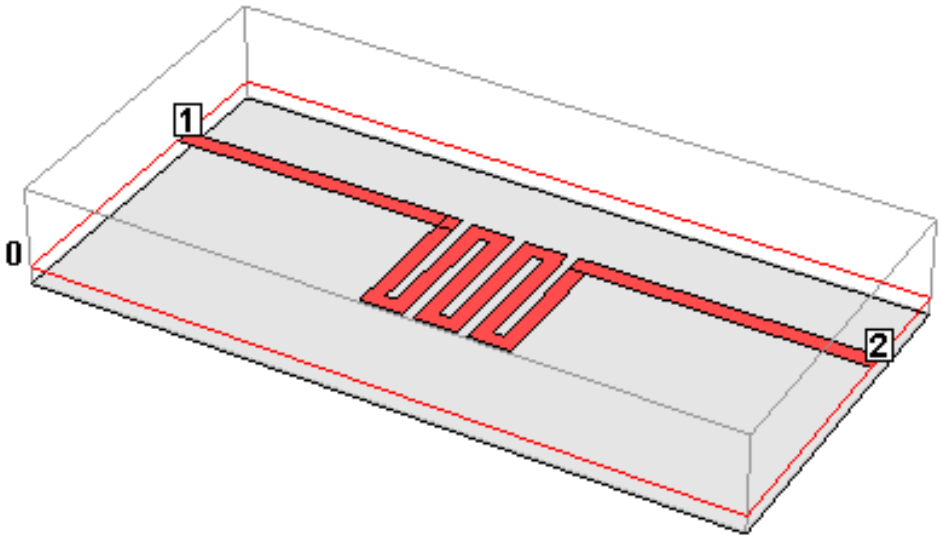

Figure 2.7 3D view of M3 in Sonnet

For the simulation, the planned frequency sweep was 50 MHz to 10 GHz with optimized meshing. However, this selection would require 48 MB of memory for calculation. Since the Lite version of Sonnet only allows the user to use up to 32 MB of memory, a less accurate but less memory hungry meshing method was selected. Instead of using Fine/Edge Meshing, Coarse/Edge Meshing was applied to obtain the results shown in Figure 2.8. By comparing the magnitude graphs of both S_{11} and S_{21} parameters with the results obtained by the previous experiments, one can observe that the trends of the curves are close with each other.

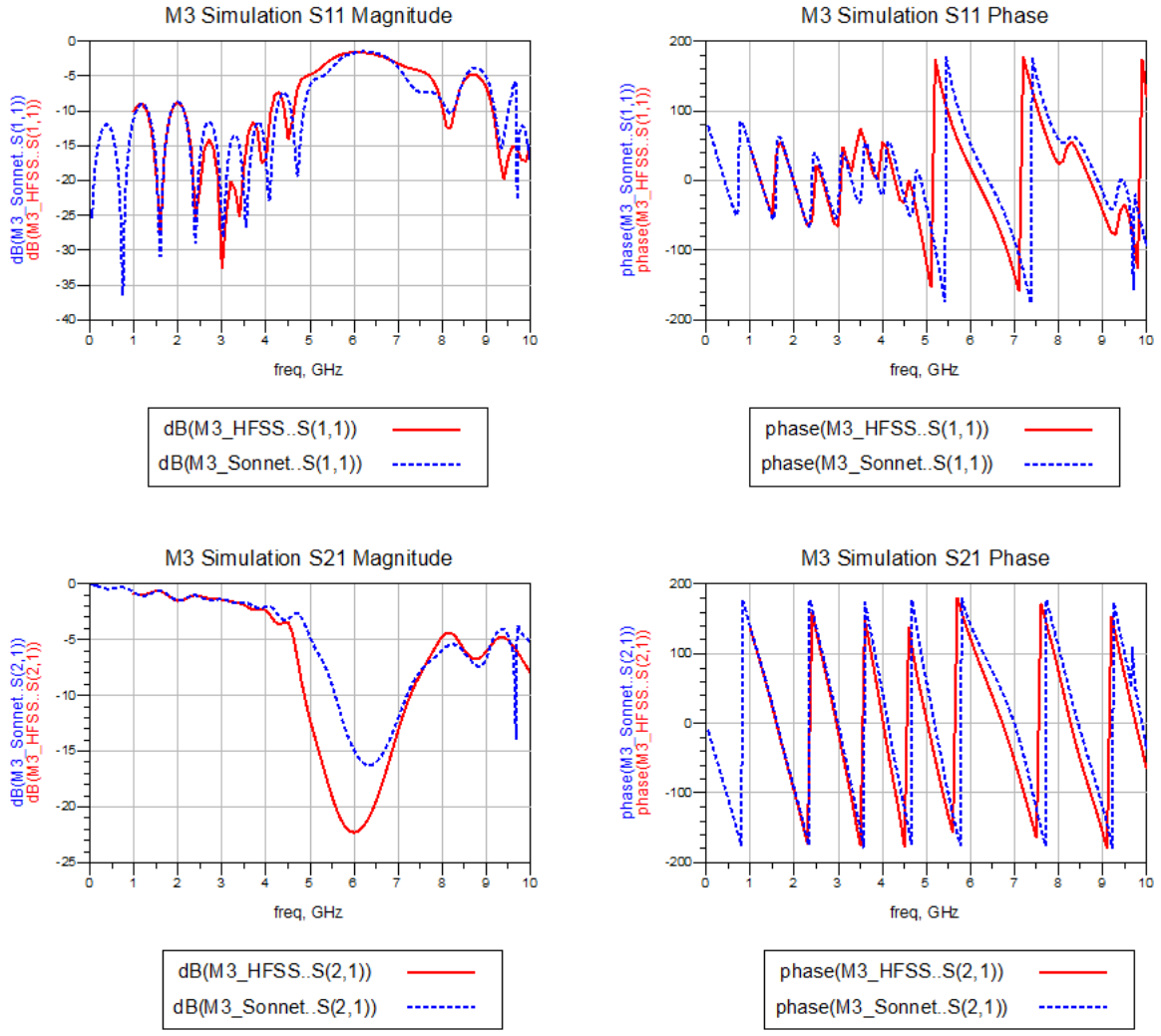

Figure 2.8 Comparison of S-parameters of M3 simulated by HFSS Designer and Sonnet

2.3 Measurement

2.3.1 Network Analyzer Calibration

In order to calibrate the network analyzers, SOLT (short, open, load, through) standards were used from the Agilent 85052D 3.5 mm calibration kit (Figure 2.9) [7]. Two network analyzers were calibrated for the measurements of M3 to ensure the uniformity of the data collected [8]. The Agilent E8358A Performance Network Analyzer in Figure 2.10 was connected to the SOLT standards directly through 3.5 mm female SMA cables with a frequency sweep of 50 MHz to 10 GHz, 601 points. The Hewlett Packard 8510C Network Analyzer in Figure 2.11 was connected to the standards with a 3.5 mm rigid SMA cable followed by a 3.5 mm to 2.4 mm connector. The setting for frequency sweep was the same as the previous one.

Figure 2.9 Agilent 85052D 3.5 mm economy calibration kit

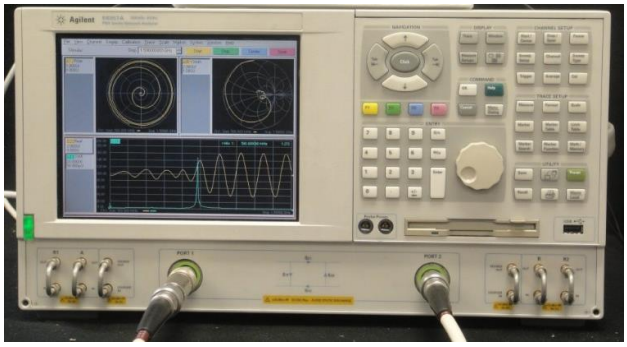

Figure 2.10 Agilent E8358A performance network analyzer

Figure 2.11 Hewlett Packard 8510C network analyzer

2.3.2 S-parameter Measurement

Based on Figure 2.12, the measurements show good correlation in the magnitudes of S_{11} and S_{21}. However, the phases of S_{21} were off by 90 degrees in the higher frequency region. To eliminate this phase shift, de-embedding of the microstrip is required because the meandered line was measured at the two connectors on the ends. Since the simulations done in section 2.1 and 2.2 did not include in the effects of the test fixture, the reference plane of the measurements has to shift to the signal lines instead of the connecters. One form of de-embedding is setting up the offset delay during the calibrations [9]. By manually adding in the electrical delays that correspond to the fixture's physical length, this difference in phase delay can be reduced. To completely resolve the discrepancy, the added electrical delay has to be an equation that varies with the effective permittivity of the materials used.

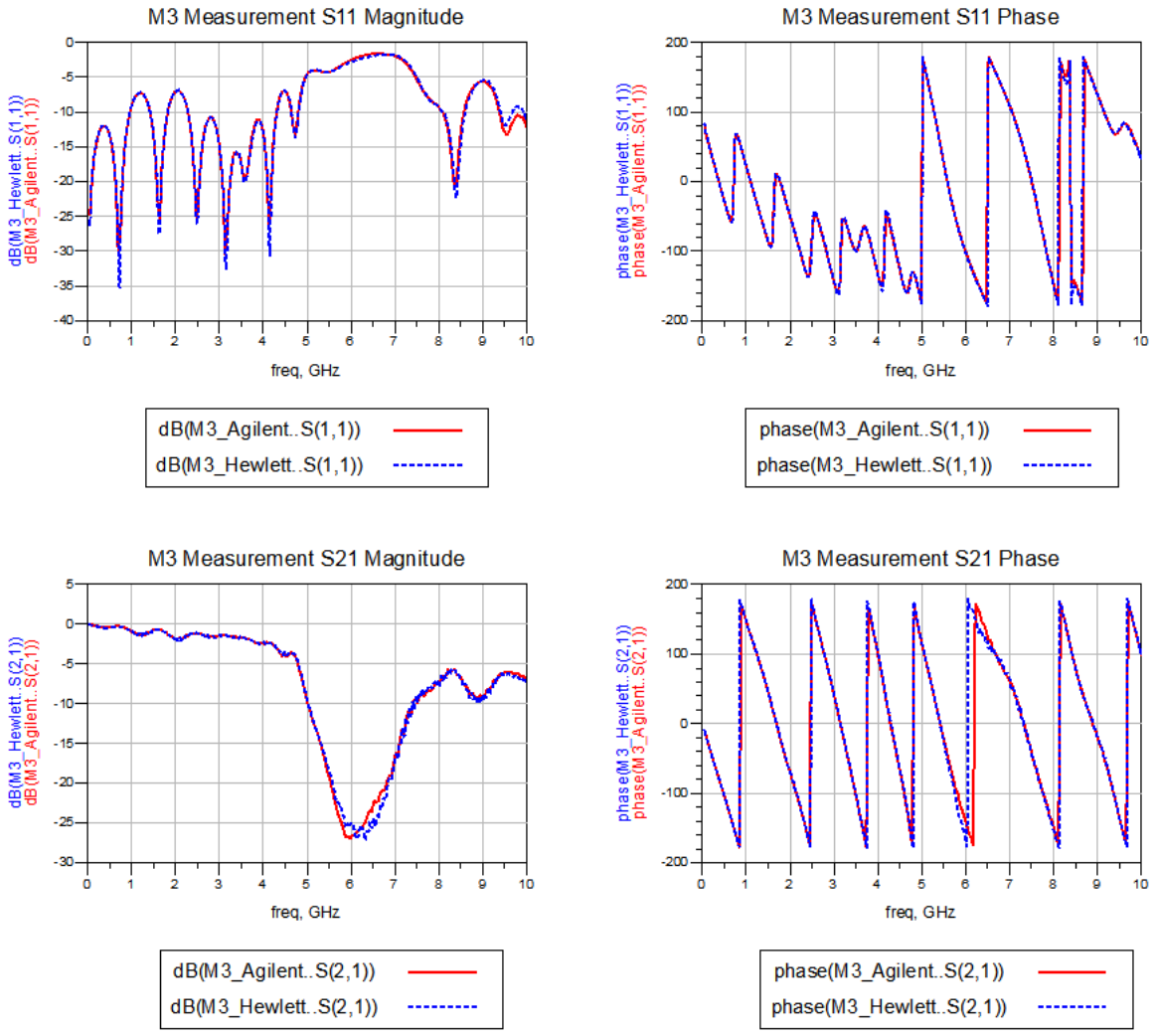

Figure 2.12 Comparison of S-parameters between M3 measured by Agilent E8358A performance network analyzer and Hewlett Packard 8510C network analyzer

2.4 Results Comparison

2.4.1 Data Export

By saving the data sets from the simulations and measurements as .s2p files, the data can be imported into Matlab with the import and read command. The intrinsic impedance used for calculation was set to 50 Ω, the same as the standard match impedance used in the measurements.

The imported frequency was then divided by 109 in order to obtain a scaled x-axis in unite of GHz. Since the S-parameter from the original data was composed as a three-dimensional matrix, the one additional dimension must be eliminated to match the plot display. Therefore, an empty two-dimensional matrix was constructed with command zeros (X, 1). Note that the number 299 of the array only applies for the imported data from Sonnet matrix. It corresponds to the points calculated in the software from the original simulation. The exact points for each import are listed in the Appendix A as the Matlab Code For Data Sets Comparison.

The results of magnitude and phase calculation for plotting y-axis (magnitudes in dB and phases in degrees) were stored in the empty two-dimensional matrix created above. The magnitude command mag2db used an absolute value before making the conversion to dB to ensure that there is no discrete value in the solution set. Phases in Figure 2.16 were extracted from the original data by taking the angle from the S-parameter and multiplying by 180/ π for the results to be in degrees. To visually compare the S-parameter values, the magnitude and phase of S_{11} and S_{21} were plotted separately with the codes in Data Display. Different colors and shapes were assigned for each data set; the legends are displayed at the bottom of the plots.

2.4.2 S-parameter Analysis

Due to precision concern, the extracted S-parameter from HFSS Designer was chosen over the Sonnet one. It is compared with the data from Hewlett Packard 8510C network analyzer to verify the correlation

between the simulation and measurement of meandered microstrip M3. As shown in Figure 2.13, good agreement is observed in the magnitude of S_{11} between the simulation and the measurement. Magnitudes of S_{21} in Figure 2.14 also agree well with each other, except that the measurement is more lossy at 6 GHz. This difference was caused by the unwanted electrical interferences (calibration, cables, etc.) that happened during the process of measuring. Similar to the de-embedding issue discussed in section 2.3.2, phases of both S_{11} and S_{22} (Figure 2.15 and 2.16) showed observable disagreement. To match and enhance the accuracy of the simulation, the Debye model is used to approximate the frequency dependent relative dielectric constant for the dielectric material. Based on the relative permittivity and loss tangent values presented in the FR-4 data sheet in Figure 2.17, a new HFSS simulation was performed and compared with the measurement data from the HP vector network analyzer (Figure 2.18).

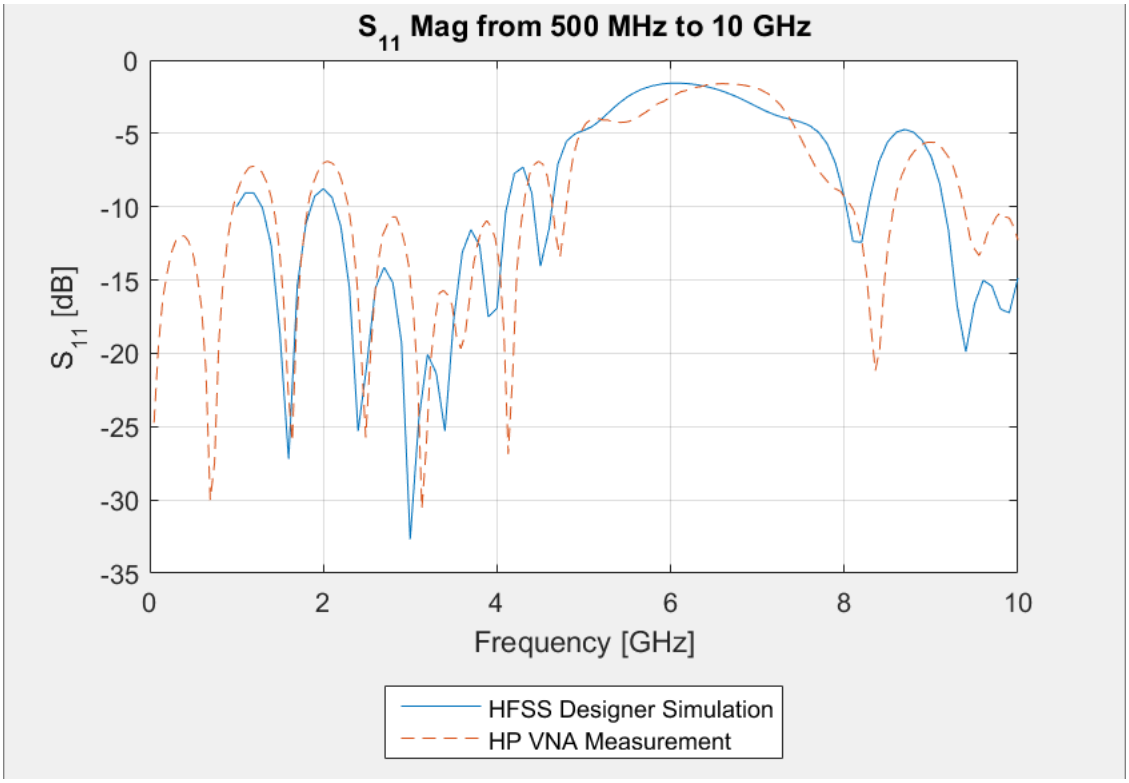

Figure 2.13 Comparison of S_{11} magnitude of M3 (HFSS Designer simulation and Hewlett Packard VNA measurement)

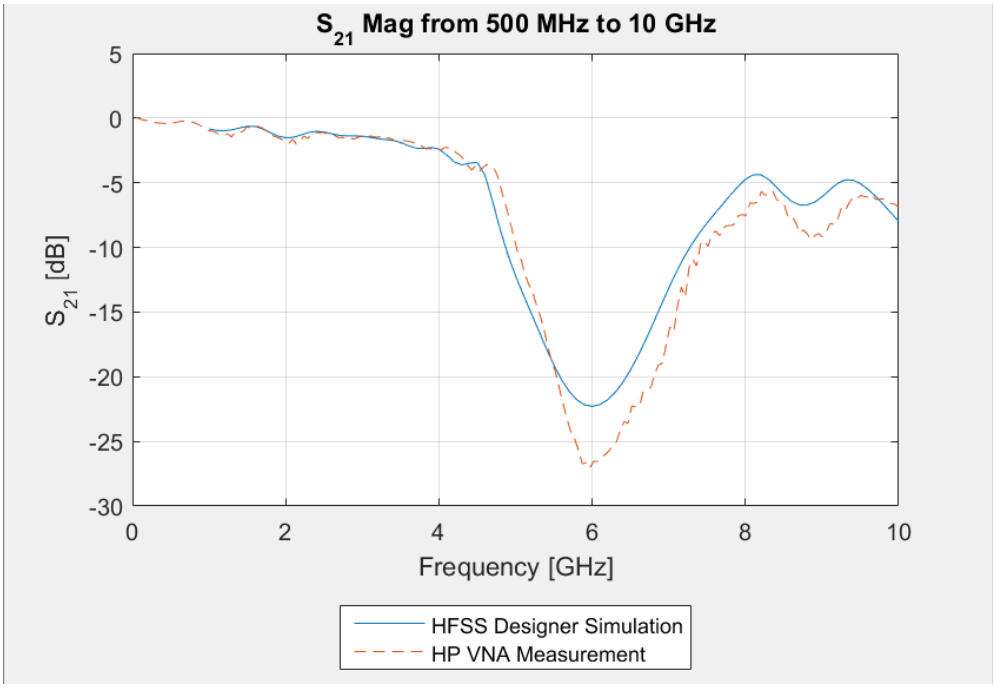

Figure 2.14 Comparison of S_{21} magnitude of M3 (HFSS Designer simulation and Hewlett Packard VNA measurement)

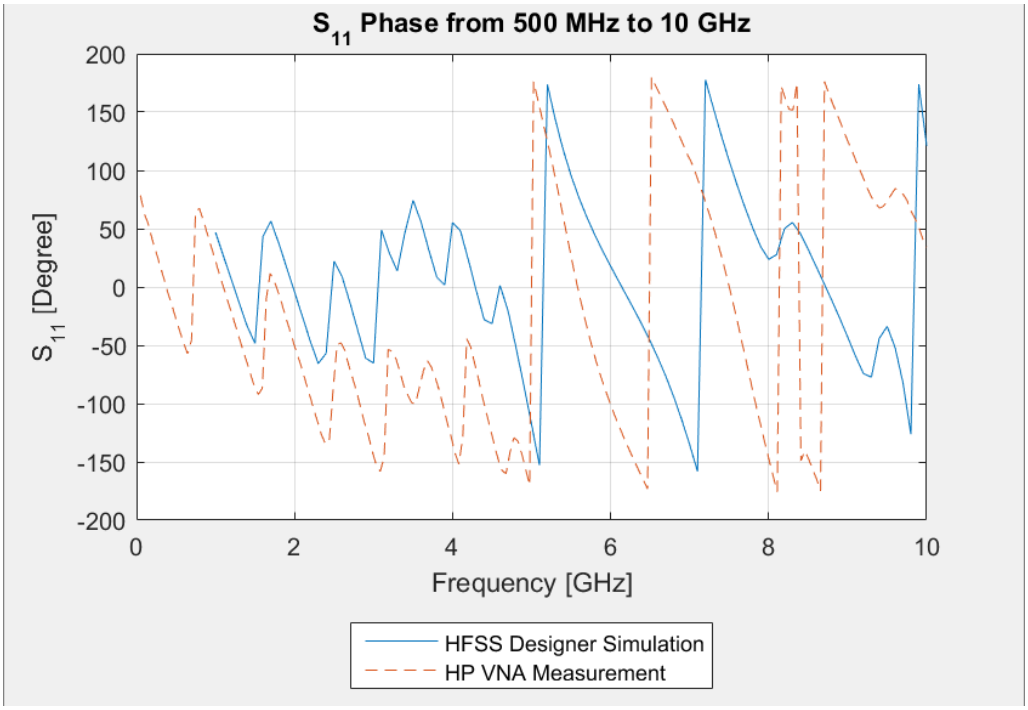

Figure 2.15 Comparison of S_{11}phase of M3 (HFSS Designer simulation and Hewlett Packard VNA measurement)

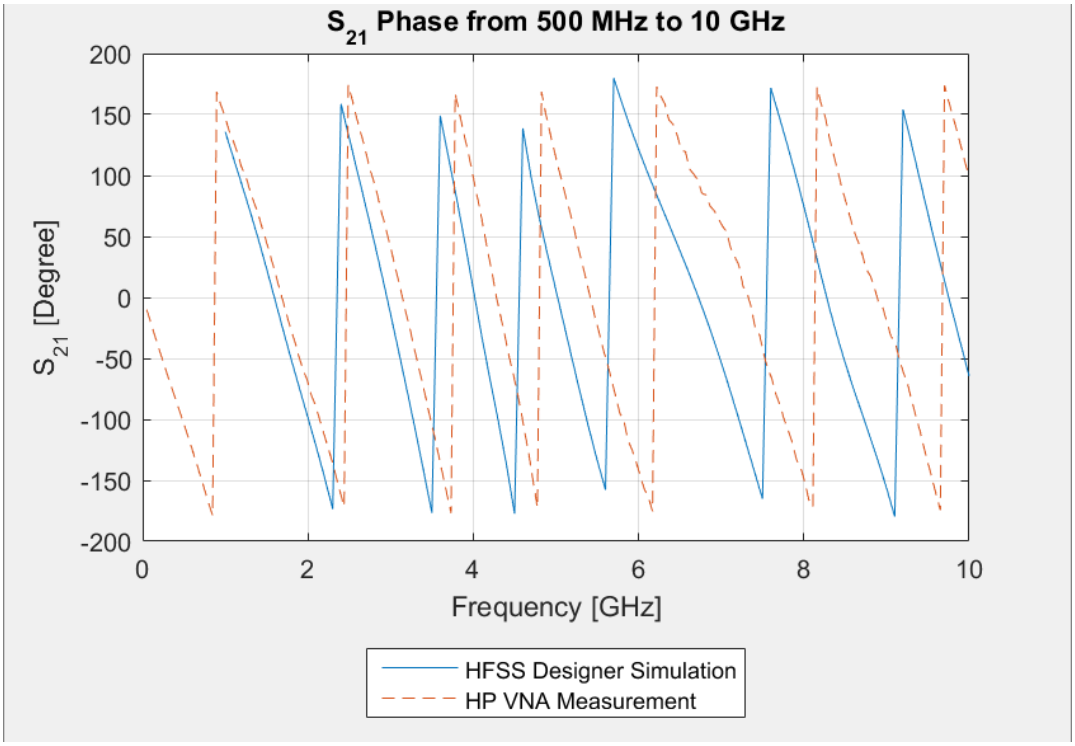

Figure 2.16 Comparison of S_{21} phase of M3 (HFSS Designer simulation and Hewlett Packard VNA measurement)

Dk, Permittivity (Laminate & prepreg as laminated) Split Post Method, Tested at 50% resin	A. @ 100 MHz B. @ 500 MHz C. @ 1 GHz D. @ 2 GHz E. @ 5 GHz	4.46 4.40 4.37 4.35 4.32
Df, Loss Tangent (Laminate & prepreg as laminated) Split Post Method, Tested at 50% resin	A. @ 100 MHz B. @ 500 MHz C. @ 1 GHz D. @ 2 GHz E. @ 5 GHz	0.020 0.021 0.022 0.023 0.024

Figure 2.17 FR-4 data sheet used for Debye model simulation

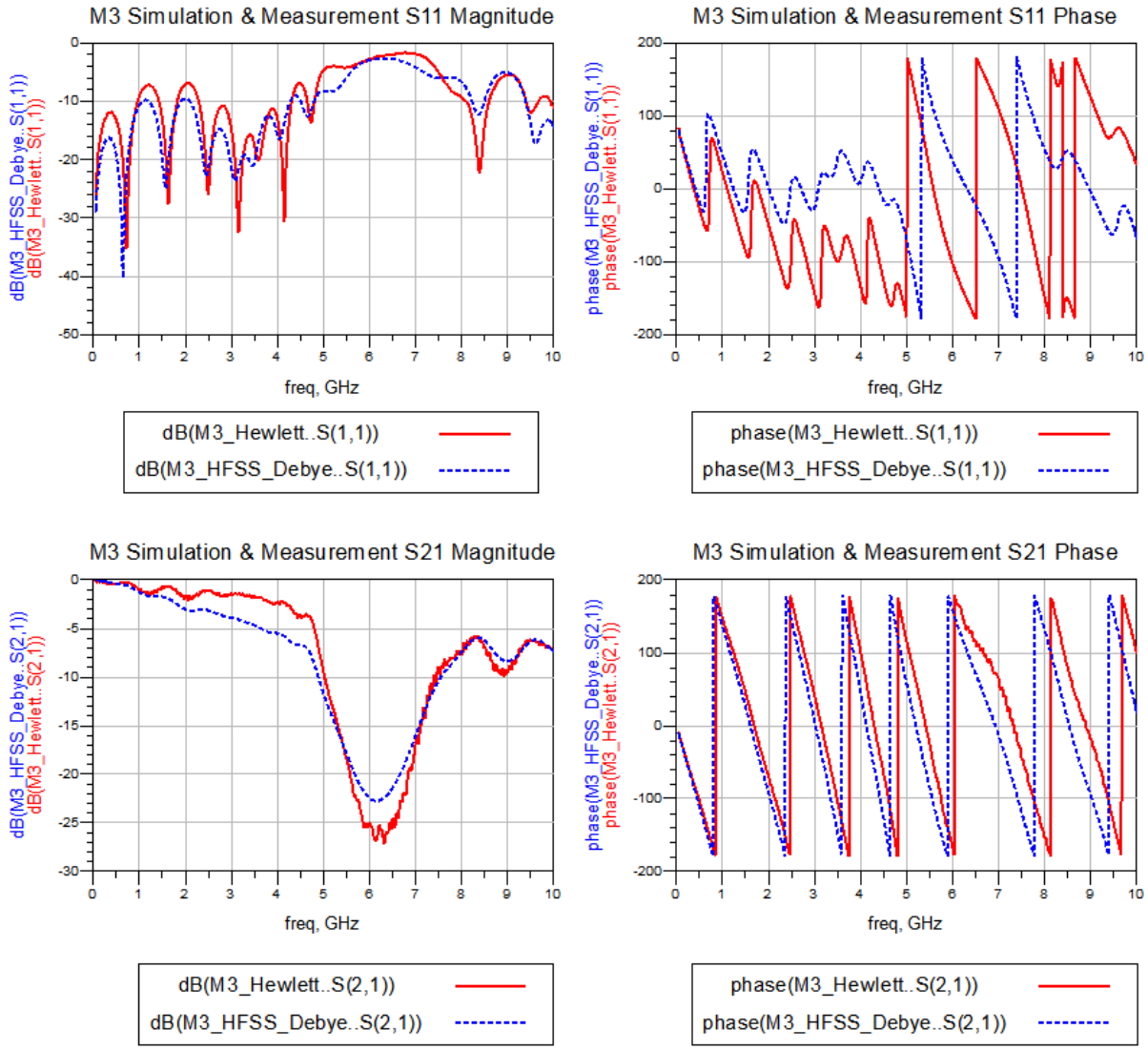

Figure 2.18 Comparison of S-parameters of M3 (HFSS Designer Debye simulation and Hewlett Packard VNA measurement)

CHAPTER 3 MICROSTRIP DESIGN AND SIMULATION

In this chapter, eight designers were designed and simulated with HFSS Designer in order to examine the changes in insertion loss associated with each design parameter of the meandered signal line. Four main categories of parameters were adjusted individually and had their S-parameters compared with the reference M3 microstrip (Design 1). Appendix B provides a detailed table of the design numbers and their corresponding top view structure.

3.1 Corner Shape

Instead of having a 1.4 mm × 1.4 mm squared shape turning corner t, Design 2 in Figure 3.1 reduces the area of the corner to half by cutting along the diagonal of the square. In total, 11.76 mm^2 of area was deducted from the original design. As for design 3 in Figure 3.2, a quarter circle of radius 1.4 mm was used as the corners, saving a space of 5.06 mm^2. The S-parameter of the designs are in Figure 3.3 shows that the 45° corner design is the least lossy one.

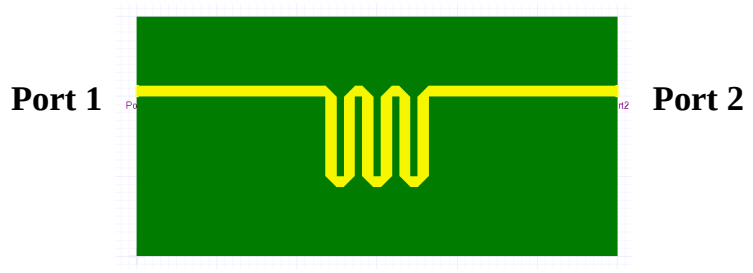

Figure 3.1 Meandered line with 45° corners (Design 2)

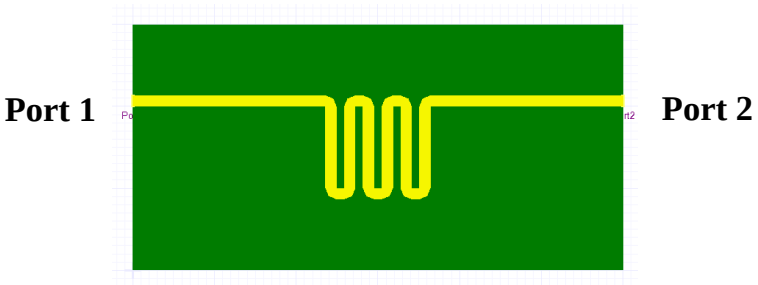

Figure 3.2 Meandered line with round corners (Design 3)

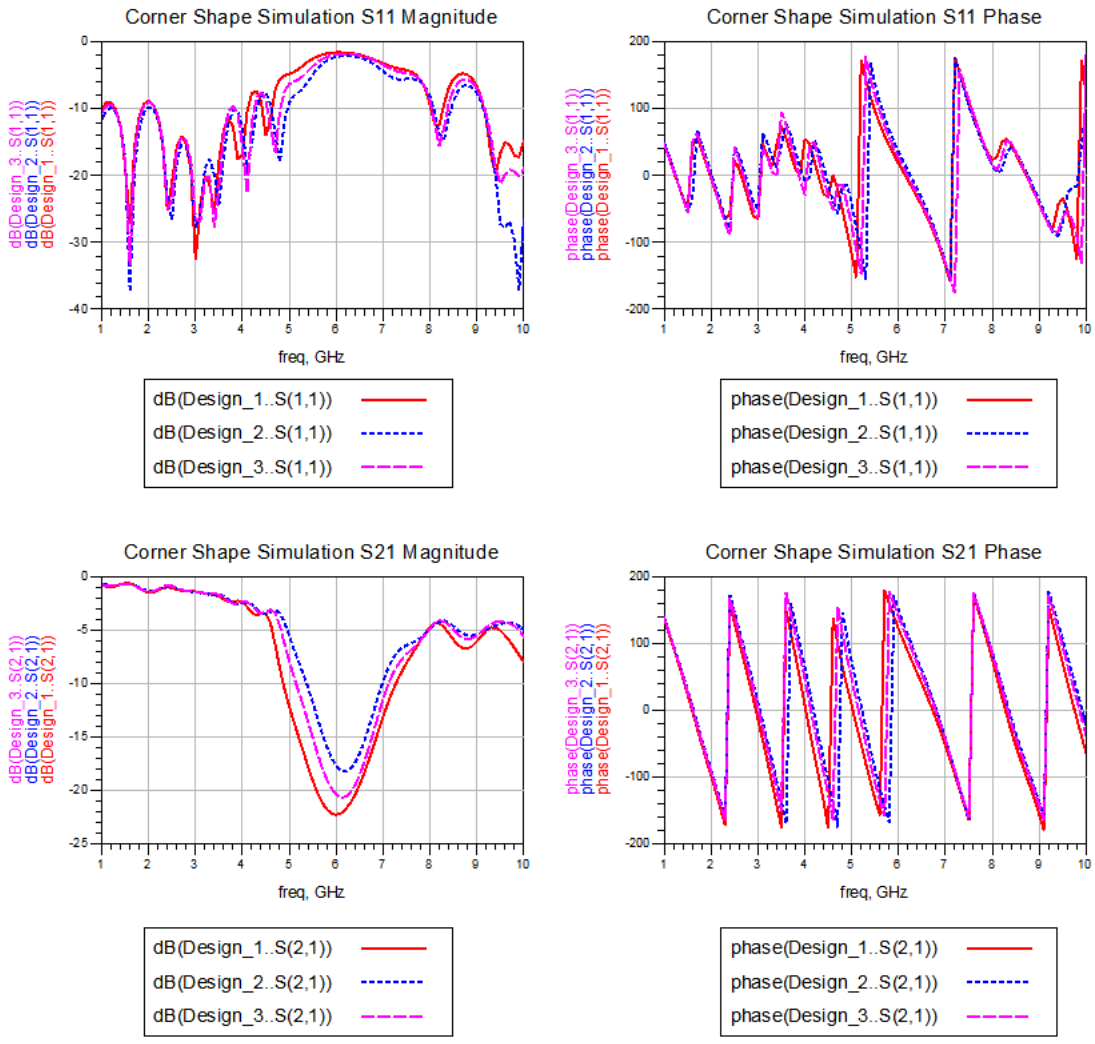

Figure 3.3 Effect of corner shape simulated with HFSS

3.2 Gap Width

Keeping the same conductor width of 1.4 mm and total length of 125 mm, the gaps in between the meandered lines were adjusted to 1.8 mm for Design 4 and 3.6 mm for Design 5 as shown in Figure 3.4 and 3.5, respectively. This increase in gap width shifts the low insertion loss region (around -5 dB) to a lower frequency as shown in Figure 3.6.

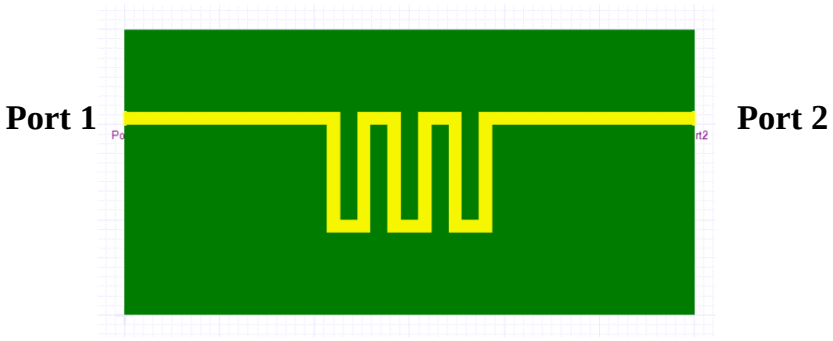

Figure 3.4 Meandered line with doubled gap width (Design 4)

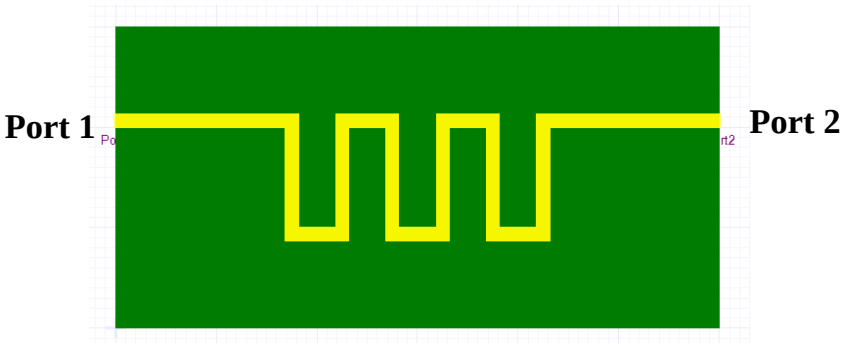

Figure 3.5 Meandered line with quadrupled gap width (Design 5)

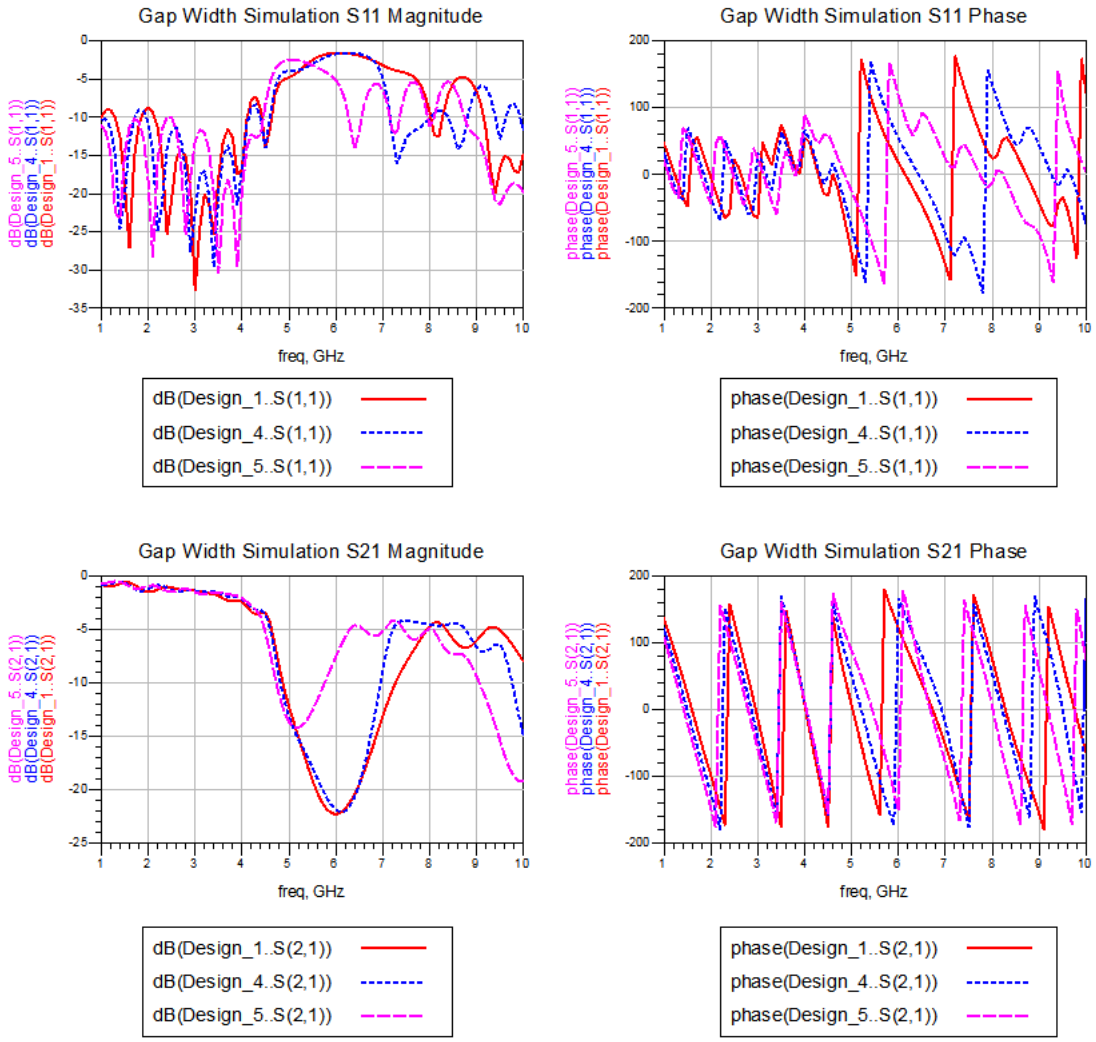

Figure 3.6 Effect of gap width simulated with HFSS

3.3 Center Corner Location

Without changing the dimensions from Design 1, Design 6 (Figure 3.7) flipped the center corner up along the center of the board. This eliminates part of the fringing field between the meandered lines thereby reducing the returning loss by 5 dB in the frequency region from 4 to 6.5 GHz (Figure 3.8).

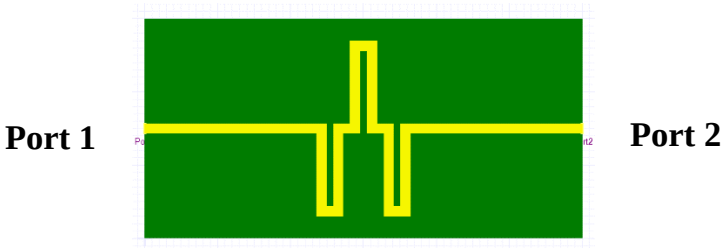

Figure 3.7 Meandered line with center corner pointed up (Design 6)

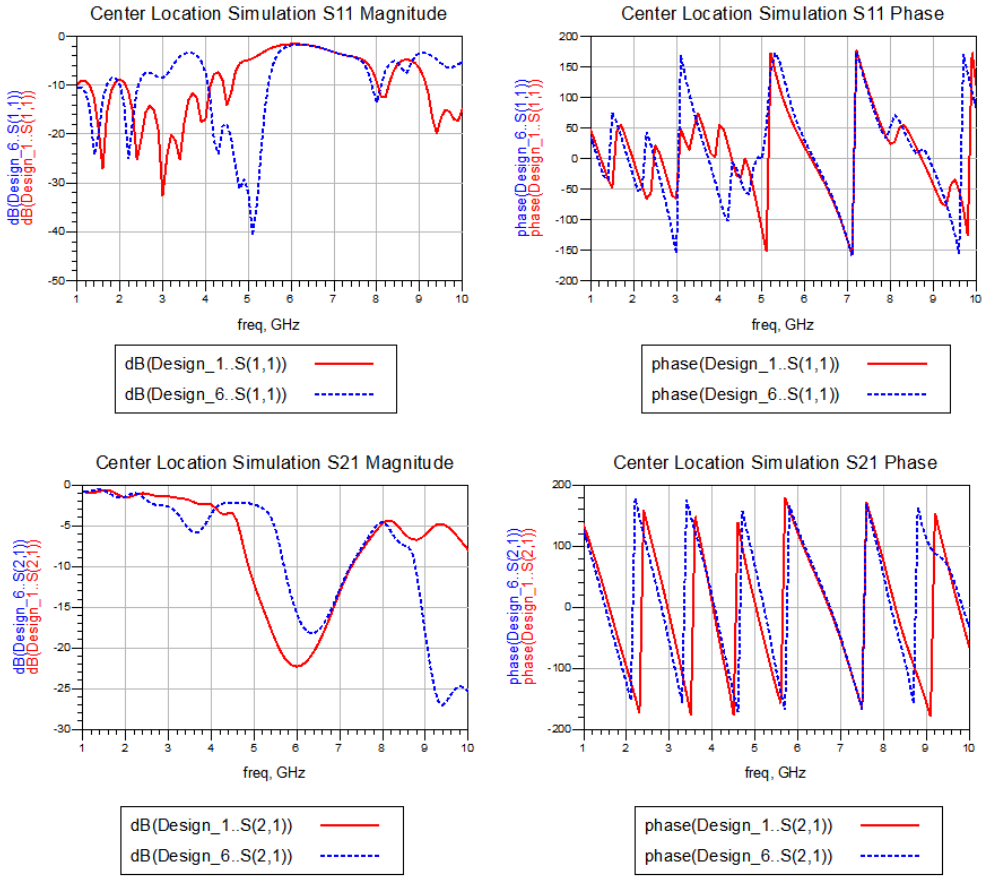

Figure 3.8 Effect of center location simulated with HFSS

3.4 Number of Legs

Design 7 (Figure 3.9) and 8 (Figure 3.10) examined the impact of having varied numbers of meandered legs. As shown in Table 3.1, both designs kept the total physical length of the original design by changing the length of the vertical strips. From the S-parameters shown in Figure 3.11, the increasing number of the legs delayed the maximum drop of insertion loss from 6 GHz of Design 1 to 8.5 GHz of Design 7 and 10 GHz of Design 8. Meanwhile, the more the meandered corners, the higher the corresponding return loss is.

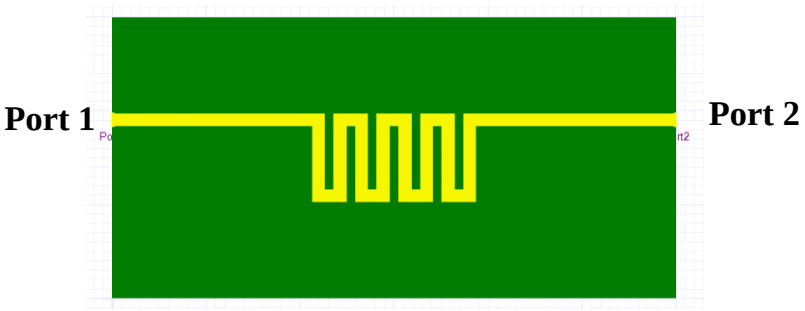

Figure 3.9 Meandered line with 4 legs (Design 7)

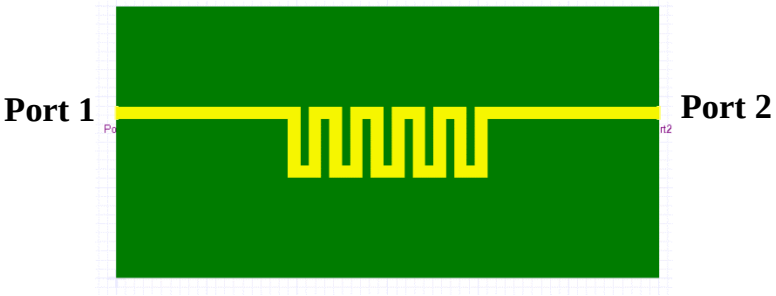

Figure 3.10 Meandered line with 5 legs (Design 8)

Table 3.1 Dimension comparison

	Design 1	Design 7	Design 8
Corners #	3	4	5
Gap Width	0.9 mm	0.9 mm	0.9 mm
Vertical Length	12. 7 mm	9.525 mm	7.9 mm
Side Length	23.55 mm	21.25 mm	18.95 mm

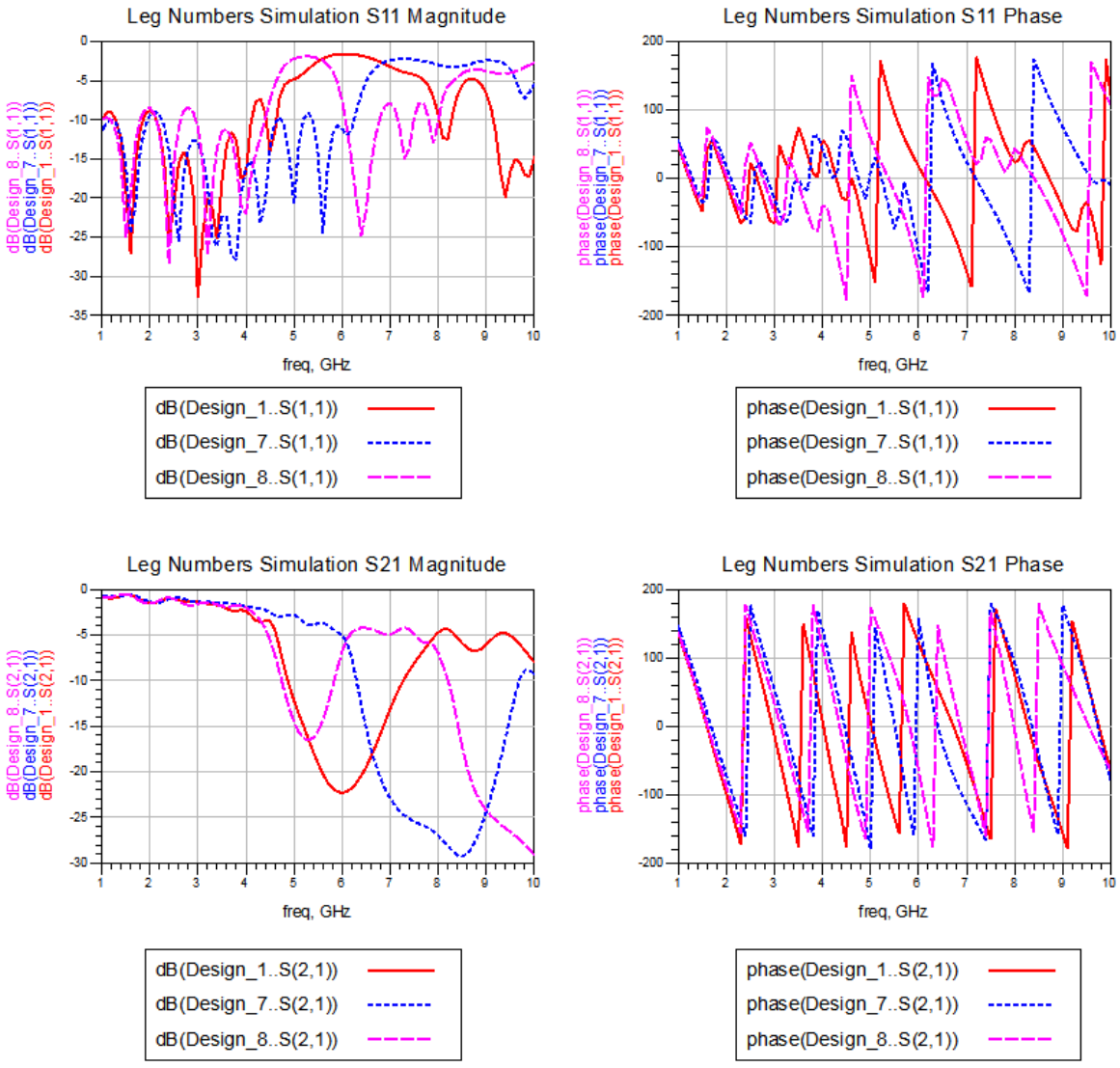

Figure 3.12 Effect of number of leg simulated with HFSS

CHAPTER 4 MEASUREMENT AND INSERTION LOSS ANALYSIS

4.1 Printed Circuit Board Fabrication

In order to fabricate all the designs in Appendix B, CadSoft EAGLE PCB Design was used to design and generate the Gerber files. Using design 6 (M3 Up) as an example, the finished board design is shown in Figure 4.1. The difference in color indicates a change in layer. The user only needs to specify the shapes in the top conductor line (layer 1) and bottom ground plane (layer 16). The software automatically defines the shape of the dielectric layer with the filling material specified. The height of these three layers can be edited in the design rule menu. After adjusting the wire width to 1.4 mm, the meandered part can be drawn by the meander tool. To adjust the length of the meander section, the total length of the line should be typed in the command. In this case, all the meandered line lengths were set to be 125 mm. In addition, besides manually locating the design, one could also type in drawing commands to enhance the figure's accuracy. For instance, the bottom copper layer in Figure 4.1 could also be done by command "layer 16 rect (0 0)(60 30)".

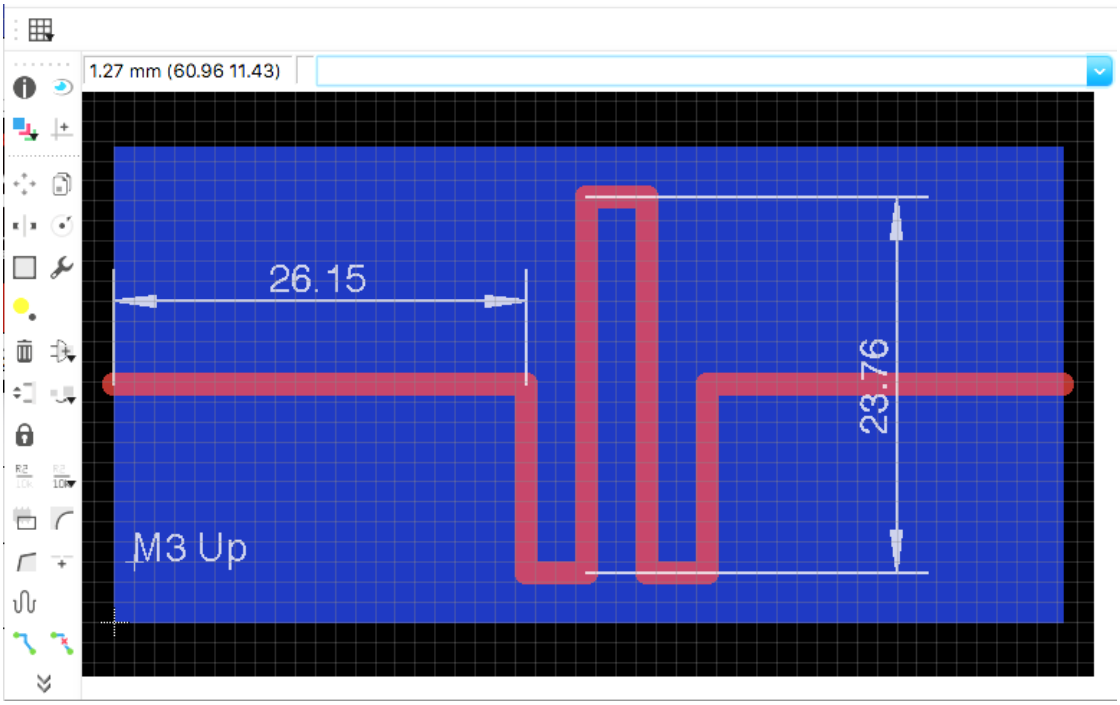

Figure 4.1 Layout of Design 6 in EAGEL

MCN Gerber Viewer in Figure 4.2 was used to ensure the quality of the files. For each variation, three files in .ger format were generated to include the information for the layers designed. These files were emailed to the ECE machine shop for fabrication. After retrieving these fabricated boards, two 3.5 mm board mount connectors were carefully soldered onto each design, connecting the ground plane with the signal line. Figures 4.3 to 4.10, correspond to designs 1 through 8 in Appendix B.

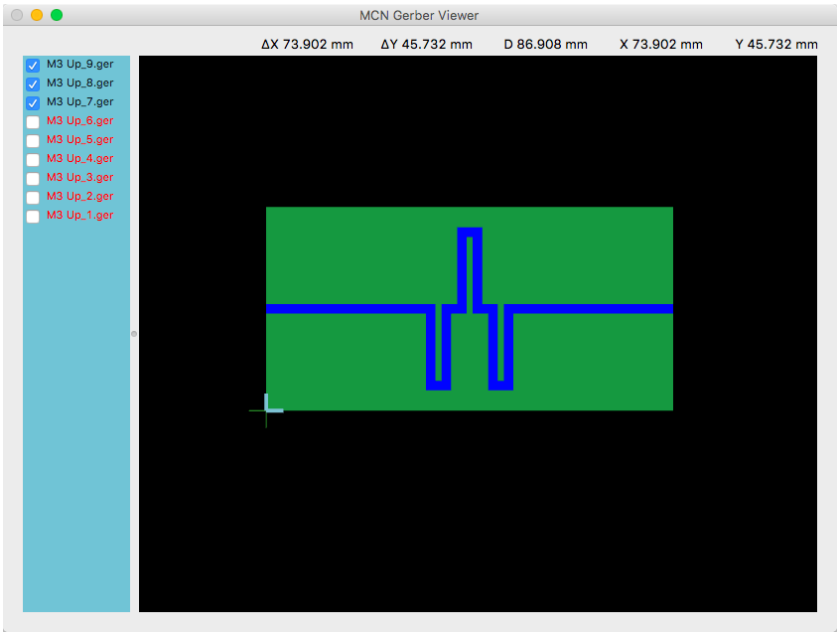

Figure 4.2 Design 6 in Gerber viewer

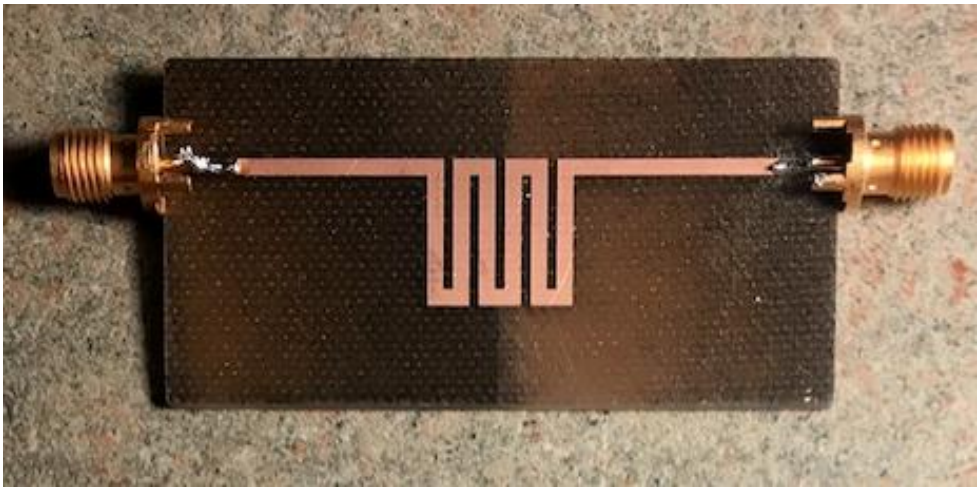

Figure 4.3 Fabricated Design 1 "Original"

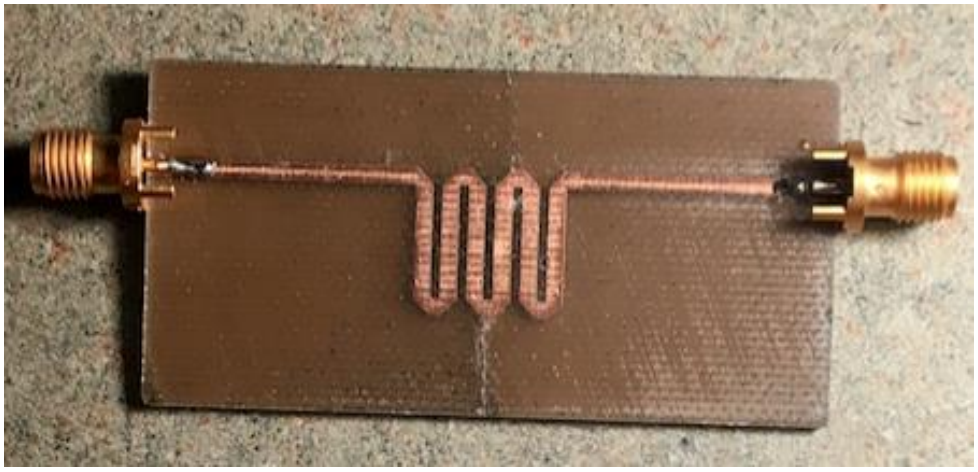

Figure 4.4 Fabricated Design 2 “M3 Angle”

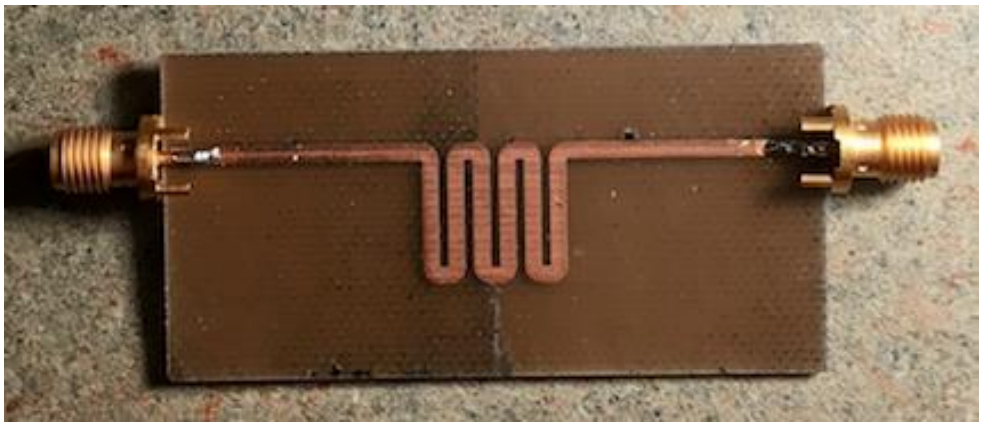

Figure 4.5 Fabricated Design 3 “M3 Round”

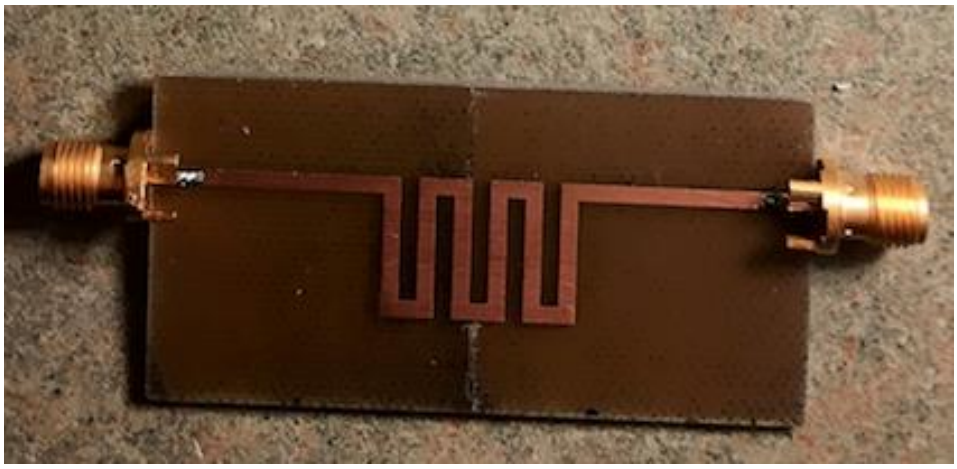

Figure 4.6 Fabricated Design 4“M3 Double Gap”

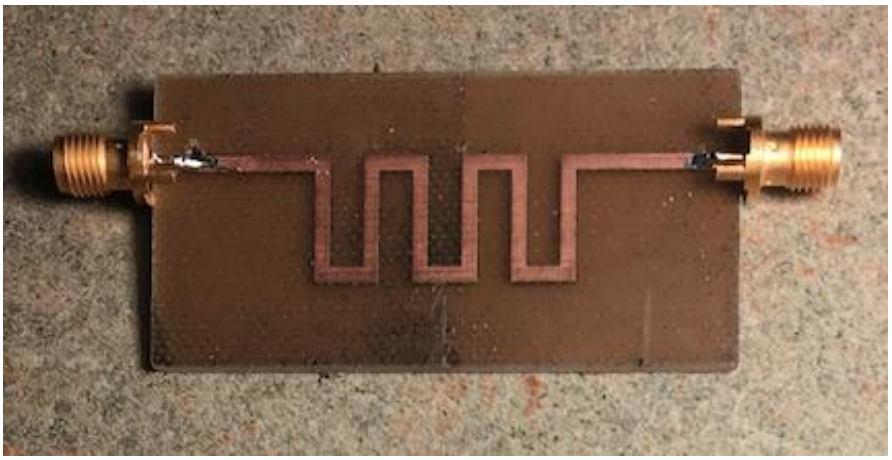

Figure 4.7 Fabricated Design 5 “M3 Four times Gap”

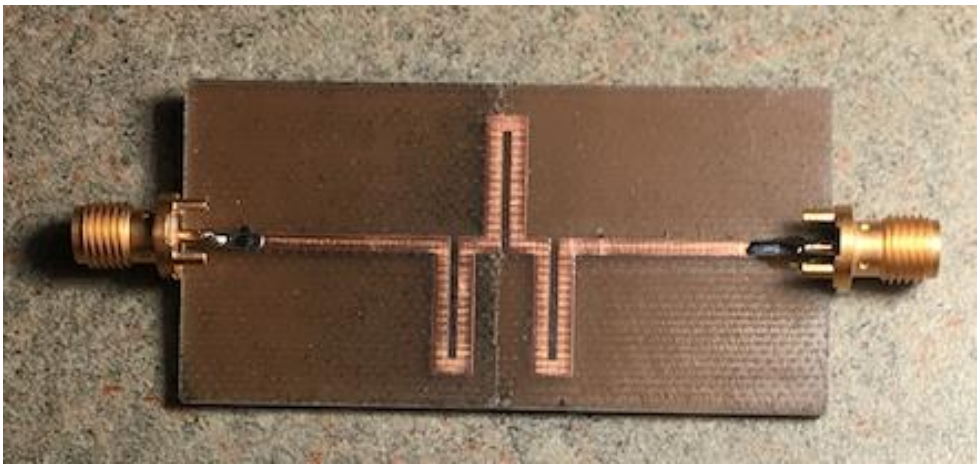

Figure 4.8 Fabricated Design 6 “M3 Up”

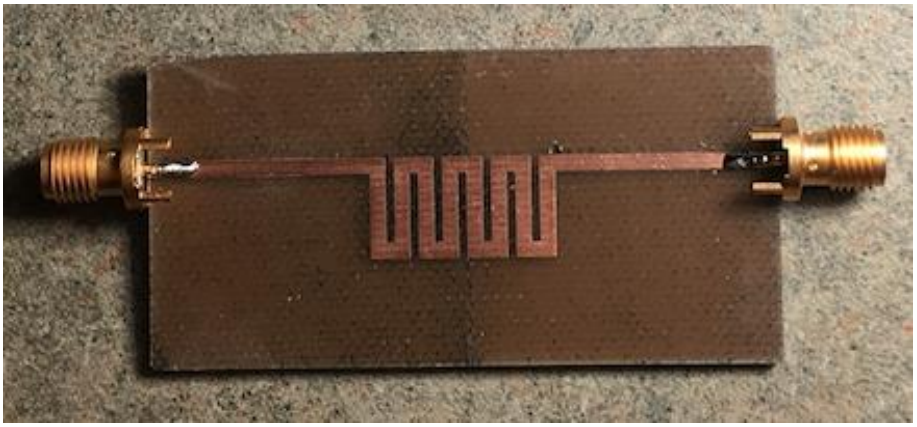

Figure 4.9 Fabricated Design 7 “M4”

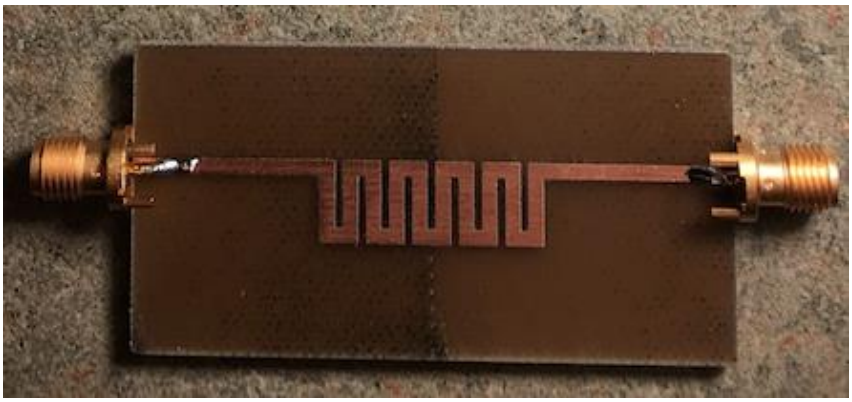

Figure 4.10 Fabricated Design 8 “M5”

4.2 S-parameter Measurement

A Hewlett Packard 8510C network analyzer, along with a 3.5 mm rigid SMA cable and a 2.4 mm to 3.5 mm connecter, was used for the measurements of the eight fabricated designs. As shown in Figure 4.11 to 4.18, the results match the simulated data very well, confirming that the relations discovered in Chapter 3 are valid and reproducible.

The only exception is Design 7, for which the magnitude of S_{21} was significantly lower in the measurement than in the simulation in the frequency region of 8 GHz to 9 GHz. A possible reason for that is the connection between the fixture and the network analyzer was not stable. To eliminate this source of error, the board was re-soldered to ensure good connection between the ground copper layer and the connectors. The device was measured again using a SOLT calibrated Agilent E8358A performance network analyzer and the resulting S-parameters are displayed in Figure 4.19. The S-parameters are plotted using linear instead of log scale to show the source of discrepancy. Since both measurement results were approaching 0 at 8.5 GHz, a difference of 0.004 in their magnitudes introduced a -20 dB difference on the log plot.

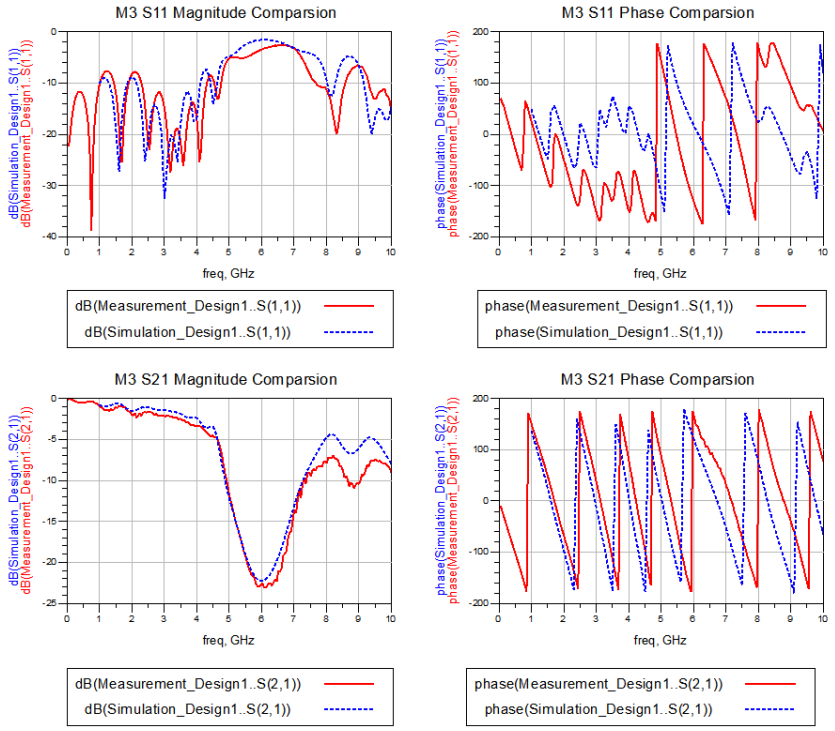

Figure 4.11 S-parameter comparison of Design 1 between HFSS simulation and measurement

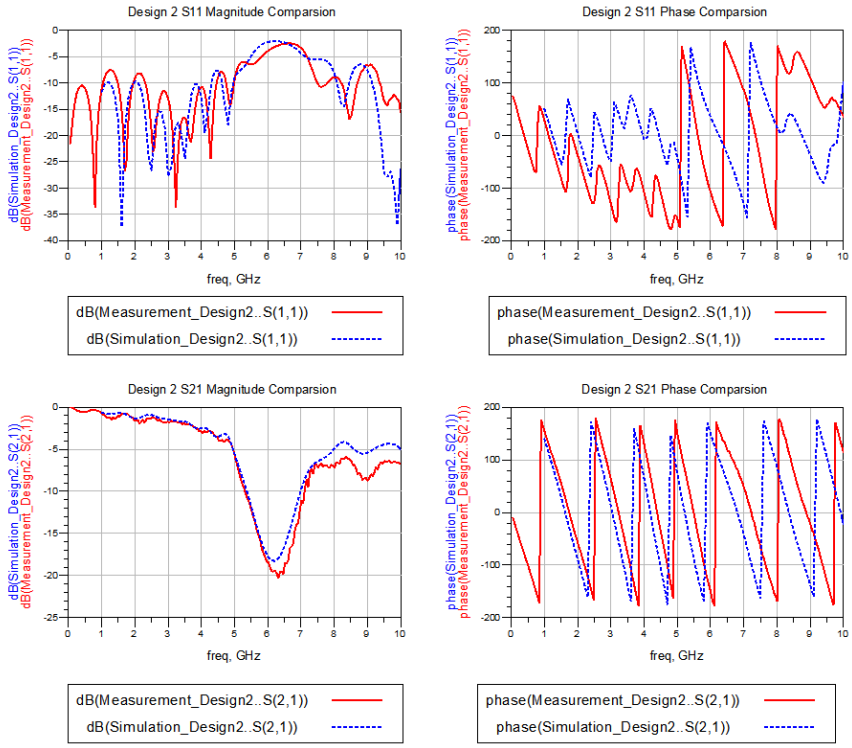

Figure 4.12 S-parameter comparison of Design 2 between HFSS simulation and measurement

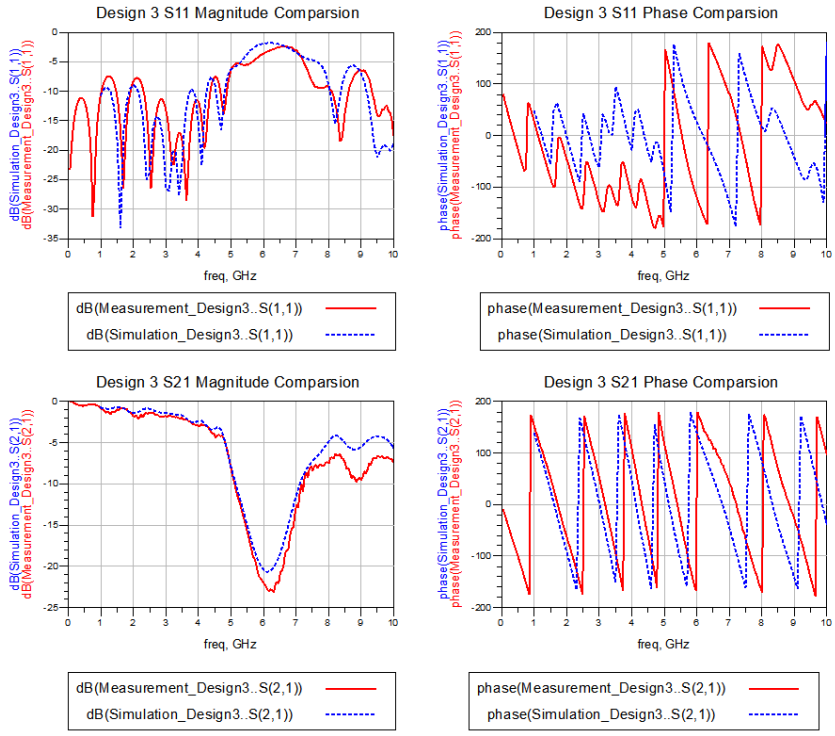

Figure 4.13 S-parameter comparison of Design 3 between HFSS simulation and measurement

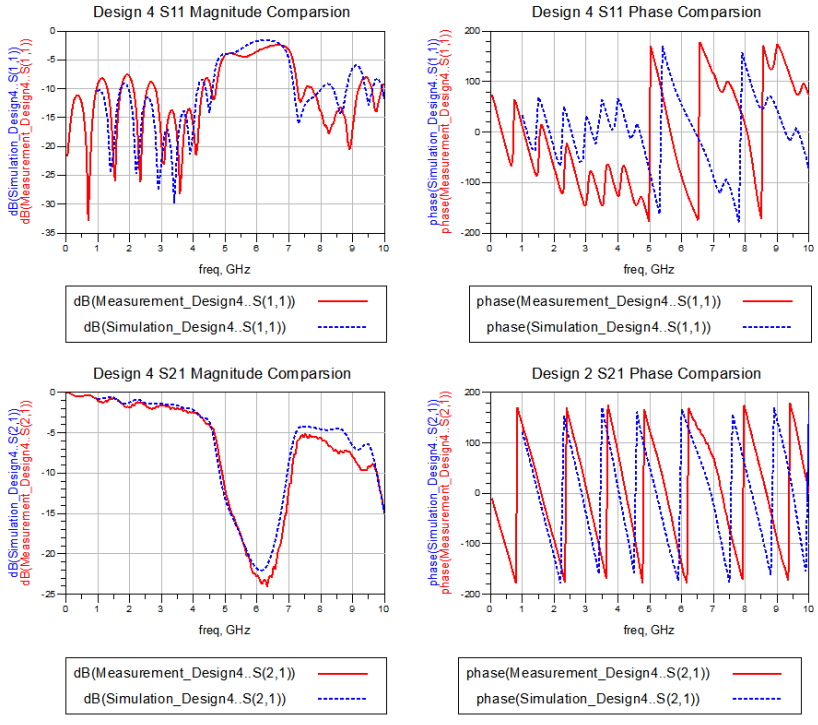

Figure 4.14 S-parameter comparison of Design 4 between HFSS simulation and measurement

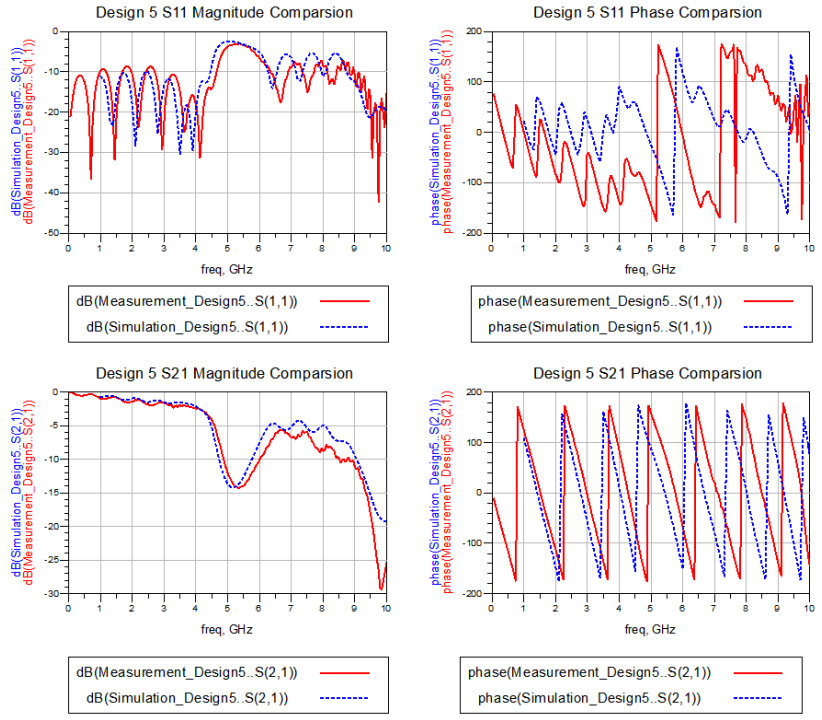

Figure 4.15 S-parameter comparison of Design 5 between HFSS simulation and measurement

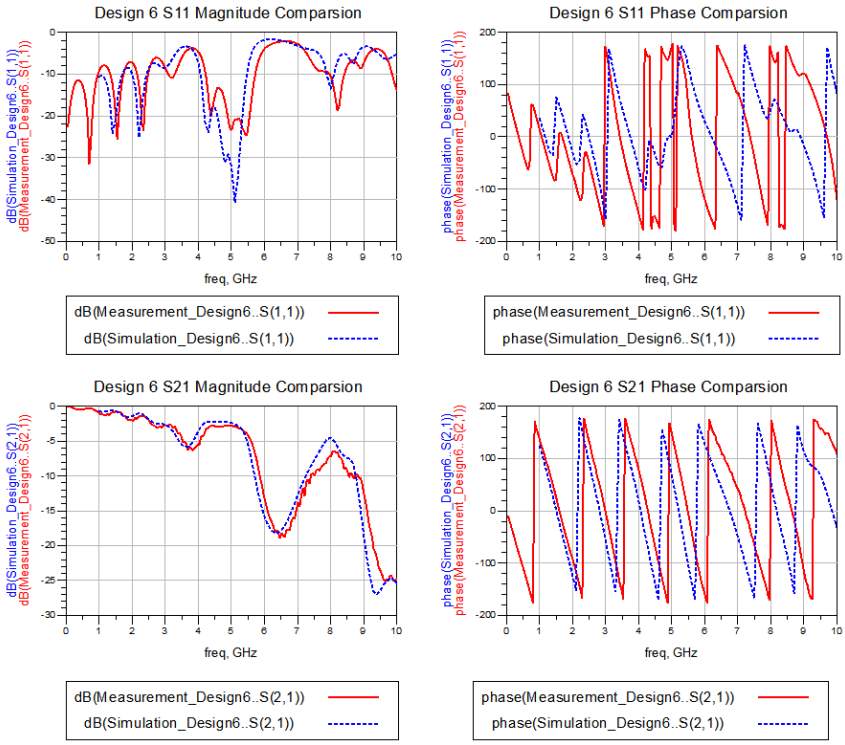

Figure 4.16 S-parameter comparison of Design 6 between HFSS simulation and measurement

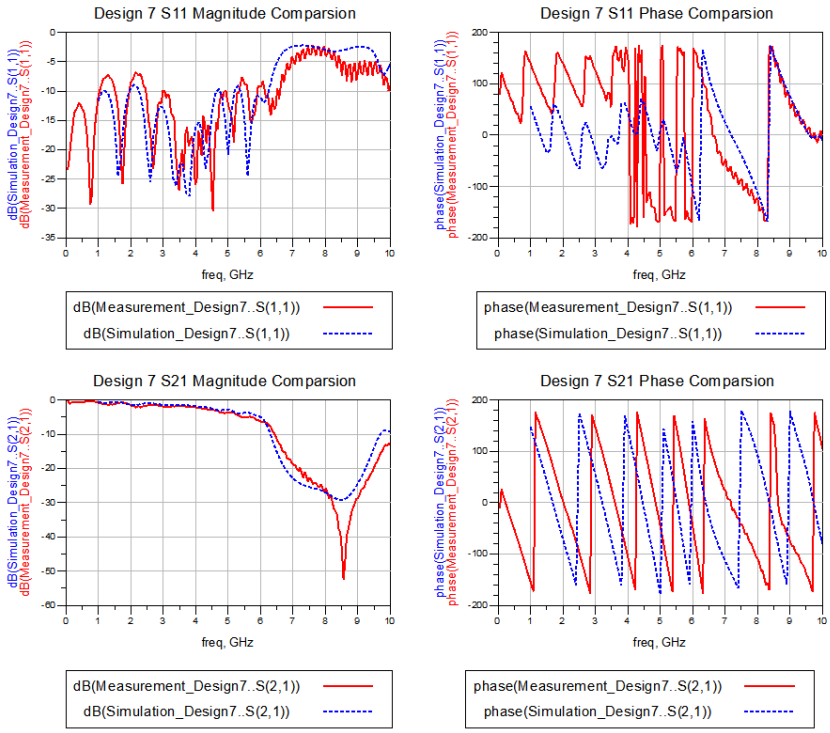

Figure 4.17 S-parameter comparison of Design 7 between HFSS simulation and measurement

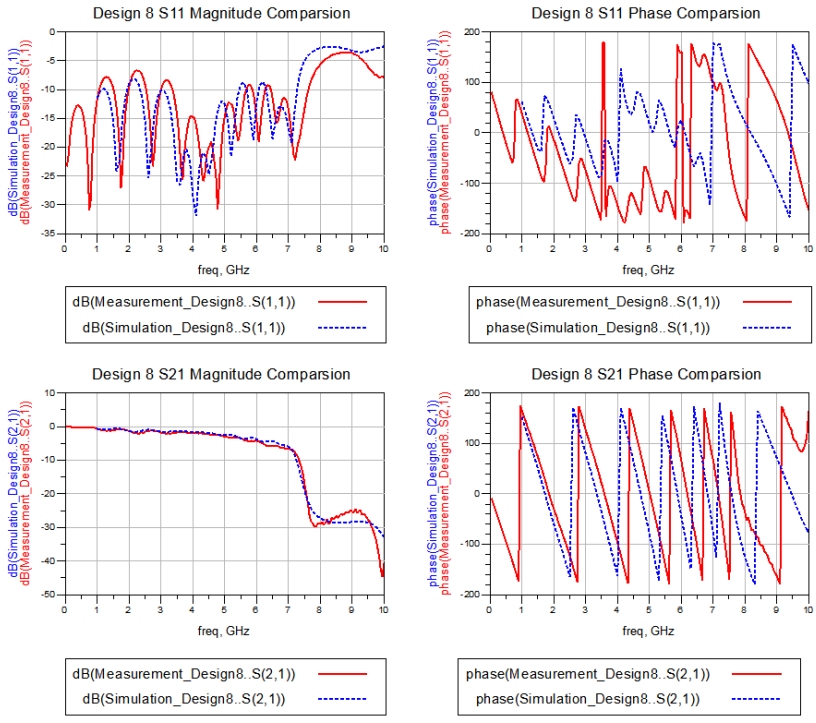

Figure 4.18 S-parameter comparison of Design 8 between HFSS simulation and measurement

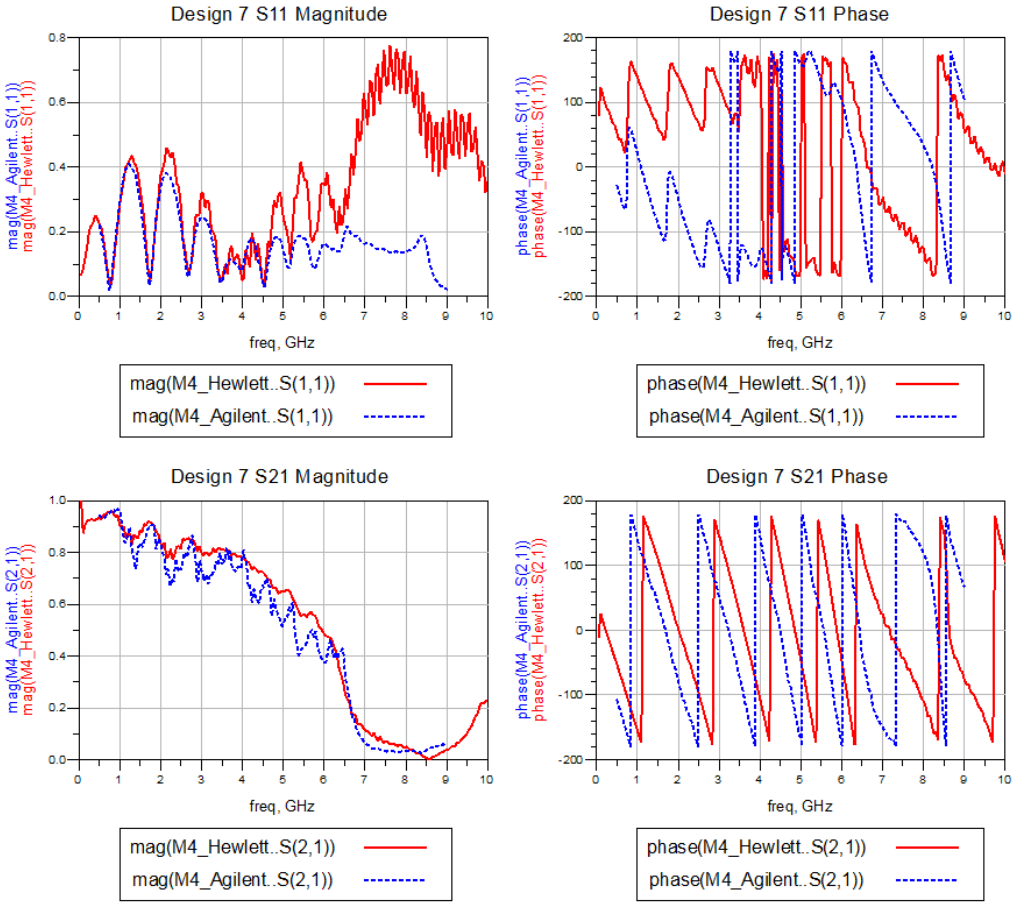

Figure 4.19 S-parameter comparison of Design 7 between Hewlett Packard 8510C and Agilent E8358A VNA measurements

CHAPTER 5 SUMMARY

The goal of this thesis was to identify the relationship between the parameters of a microstrip meandered line and their corresponding effect on the network's insertion loss. From the RF simulations in Chapter 3, it is clear that while maintaining the same physical and electrical length, the insertion loss of a microstrip can be manipulated by deliberately alternating the meandered line's corner shape, gap width, center location and meandered corner numbers. It is also shown in Chapter 4 that the measurement results mostly agree with the conclusions from the HFSS simulations. To obtain the optimized correlation between the data sets, the characterization of the microstrips should also take into consideration the fiber weave effects [10] and the electrical delays introduced by the connectors.

Future work will examine the effects of combining multiple features into one design. In order to do this, the procedure flowchart in Figure 5.1 should be followed. Assuming the new design combines the effects that correspond to each feature, an EM model of the new microstrip will be constructed and simulated. After validating the assumption with the simulation results, measurements from the fabricated design will be used to further complete the theory.

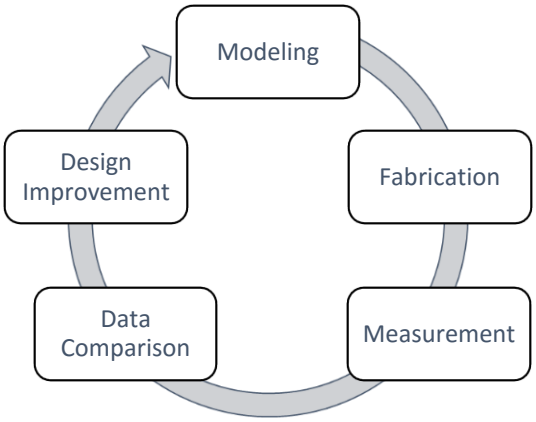

Figure 5.1 Workflow for the future work on the performance analysis of the meandered-line microstrips

REFERENCES

[1] A.R. Djordjevi, M.D. Djuri, D.V. To˘si , and T.K. Sarkar. On compact printed-circuit transmission lines. Microwave and Optical Technology Letters, 49(11): 2706–2709, 2007.

[2] M. Ali and T. Abbas. Compact, meandered-line microstrip bandpass filter. In Multi-Topic Conference (INMIC), 2014 IEEE 17th International, pages 67–72, Dec 2014.

[3] D. Kumar and A.De. Effective size reduction technique for microstrip filters. Journal of Electromagnetic Analysis and Applications, 05(04): 166–174, 2013.

[4] J. Jin, Theory and computation of electromagnetic fields. Hoboken, N.J.: Wiley, 2010.

[5] ANSYS, Inc, Ansys Designer RF Brochure14.0. Resource Library MKT 105, Dec 2011.

[6] Sonnet Software, Inc, Efficient Meshing in Sonnet 1S.0. Technical Resource Documents, 2008.

[7] Agilent Technologies, Agilent AN 154 S-parameter Design. Application Note 5952-1087, 2005.

[8] Agilent Technologies, PNA Series Network Analyzers Printed Version of PNA Help User's and Programming Guide. Application Note A.08.00, 2008.

[9] Agilent Technologies, De-embedding and Embedding S-parameter Networks Using a Vector Network Analyzer, ser. Application Note 1364-1, 2000.

[10] T. Zhang, X. Chen, J. E. Schutt-Ainé and A. C. Cangellaris, Statistical analysis of fiber weave effect over differential microstrips on printed circuit boards, In Signal and Power Integrity (SPI), 2014 IEEE 18th Workshop on, Ghent, 2014, pp. 1-4.

APPENDIX A. MATLAB CODE FOR DATA SETS COMPARISON

```
Z0 = 50;

SonnetImport = 'Sonnet.s2p';
SonnetData = read (rfdata.data,SonnetImport);
Sonnetfreq = SonnetData.Freq / (10^9);
SonnetS = extract (SonnetData,'S_PARAMETERS',Z0);
SonnetS11 = zeros(299,1);
SonnetS21 = zeros(299,1);
SonnetS11A = zeros(299,1);
SonnetS21A = zeros(299,1);
SonnetS11(:,1) = mag2db(abs(SonnetS(1,1,:)));
SonnetS21(:,1) = mag2db(abs(SonnetS(2,1,:)));
SonnetS11A(:,1) = angle(SonnetS(1,1,:))*180/pi;
SonnetS21A(:,1) = angle(SonnetS(2,1,:))*180/pi;

HFSSImport = 'HFSS.s2p';
HFSSData = read (rfdata.data,HFSSImport);
HFSSfreq = HFSSData.Freq / (10^9);
HFSSS = extract (HFSSData,'S_PARAMETERS',Z0);
HFSSS11 = zeros(100,1);
HFSSS21 = zeros(100,1);
HFSSS11A = zeros(100,1);
HFSSS21A = zeros(100,1);
HFSSS11(:,1) = mag2db(abs(HFSSS(1,1,:)));
HFSSS21(:,1) = mag2db(abs(HFSSS(2,1,:)));
HFSSS11A(:,1) = angle(HFSSS(1,1,:))*180/pi;
HFSSS21A(:,1) = angle(HFSSS(2,1,:))*180/pi;

EMImport = 'EM.s2p';
EMData = read (rfdata.data,EMImport);
EMfreq = EMData.Freq / (10^9);
EMS = extract (EMData,'S_PARAMETERS',Z0);
EMS11 = zeros(91,1);
EMS21 = zeros(91,1);
EMS11A = zeros(91,1);
EMS21A = zeros(91,1);
EMS11(:,1) = mag2db(abs(EMS(1,1,:)));
EMS21(:,1) = mag2db(abs(EMS(2,1,:)));
EMS11A(:,1) = angle(EMS(1,1,:))*180/pi;
EMS21A(:,1) = angle(EMS(2,1,:))*180/pi;

M3Import = 'M3.s2p';
M3Data = read (rfdata.data,M3Import);
M3freq = M3Data.Freq / (10^9);
M3S = extract (M3Data,'S_PARAMETERS',Z0);
M3S11 = zeros(201,1);
M3S21 = zeros(201,1);
M3S11A = zeros(201,1);
M3S21A = zeros(201,1);
M3S11(:,1) = mag2db(abs(M3S(1,1,:)));
M3S21(:,1) = mag2db(abs(M3S(2,1,:)));
M3S11A(:,1) = angle(M3S(1,1,:))*180/pi;
M3S21A(:,1) = angle(M3S(2,1,:))*180/pi;
```

```
M10Import = 'M10.s2p';
M10Data = read (rfdata.data,M10Import);
M10freq = M10Data.Freq / (10^9);
M10S = extract (M10Data,'S_PARAMETERS',Z0);
M10S11 = zeros(201,1);
M10S21 = zeros(201,1);
M10S11A = zeros(201,1);
M10S21A = zeros(201,1);
M10S11(:,1) = mag2db(abs(M10S(1,1,:)));
M10S21(:,1) = mag2db(abs(M10S(2,1,:)));
M10S11A(:,1) = angle(M10S(1,1,:))*180/pi;
M10S21A(:,1) = angle(M10S(2,1,:))*180/pi;


figure
plot(Sonnetfreq,SonnetS11,HFSSfreq,HFSSS11,EMfreq,EMS11,M3freq,M3S11,M
10freq,M10S11);
grid on
title('S_{11} Mag from 500 MHz to 10 GHz');
xlabel('Frequency [GHz]');
ylabel('S_{11} [dB]');
legend('Sonnet Simulation','HFSS Simulation','3D Layout Simulation','3
Terms Error Correction','10 Terms Error
Correction','Location','southoutside');

figure
plot(Sonnetfreq,SonnetS21,HFSSfreq,HFSSS21,EMfreq,EMS21,M3freq,M3S21,M
10freq,M10S21);
grid on
title('S_{21} Mag from 500 MHz to 10 GHz');
xlabel('Frequency [GHz]');
ylabel('S_{21} [dB]');
legend('Sonnet Simulation','HFSS Simulation','3D Layout Simulation','3
Terms Error Correction','10 Terms Error
Correction','Location','southoutside');

figure
plot(Sonnetfreq,SonnetS11A,HFSSfreq,HFSSS11A,EMfreq,EMS11A,M3freq,M3S1
1A,M10freq,M10S11A);
grid on
title('S_{11} Phase from 500 MHz to 10 GHz');
xlabel('Frequency [GHz]');
ylabel('S_{11} [Degree]');
legend('Sonnet Simulation','HFSS Simulation','3D Layout Simulation','3
Terms Error Correction','10 Terms Error
Correction','Location','southoutside');

figure
plot(Sonnetfreq,SonnetS21A,HFSSfreq,HFSSS21A,EMfreq,EMS21A,M3freq,M3S2
1A,M10freq,M10S21A);
grid on
title('S_{21} Phase from 500 MHz to 10 GHz');
xlabel('Frequency [GHz]');
ylabel('S_{21} [Degree]');
legend('Sonnet Simulation','HFSS Simulation','3D Layout Simulation','3
Terms Error Correction','10 Terms Error
Correction','Location','southoutside');
```

APPENDIX B. DESIGN SUMMARY

Design No.	HFSS Layout	Fabricated PCB	Varied Parameter	Parameter Value
1	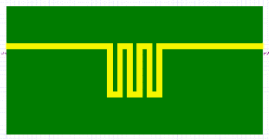		/	/
2			Corner Angle	r = 1.4 mm (45°) 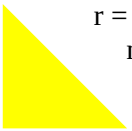
3	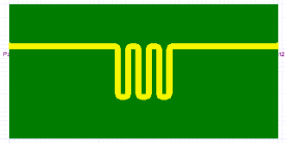	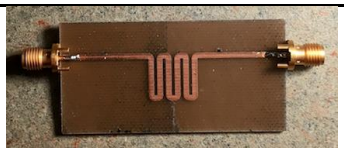	Corner Angle	r = 1.4mm
4			Gap Width	0.9 mm x 2 = 1.8 mm
5	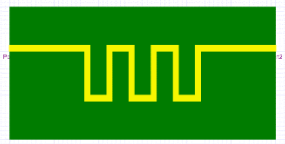	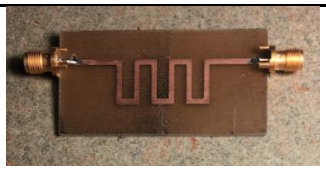	Gap Width	0.9 mm x 4 = 3.6 mm
6	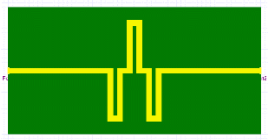	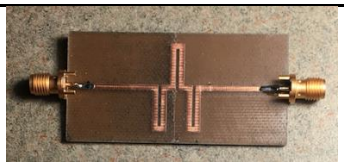	Center U Shape Location	Down → Up
7		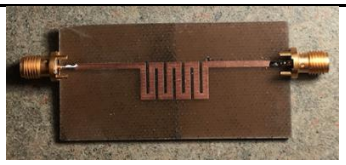	Number Of Legs	3 → 4
8	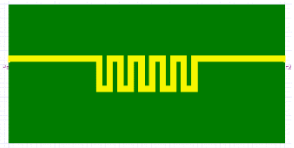	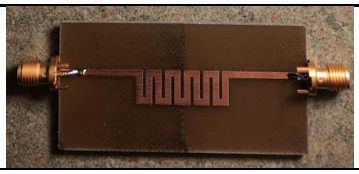	Number Of Legs	3 → 5